tion, nuclear exclusion, and inhibition of FOXO and in reentry of cells into the cell cycle as a consequence of the loss of the effects of FOXO on the expression of these target genes.

FOXO also plays a role in G_2 phase of the cell cycle. Ectopic expression or conditional expression of a constitutively active form of FOXO induces G_2 delay or G_2 arrest in addition to G_1 arrest (20, 66). DNA microarray analysis has implicated GADD45a (growth arrest– and DNA damage–inducible protein a of 45 kDa) as a potential mediator of G_2 arrest induced by FOXO activation (20, 66). A role for GADD45a in G_2-M checkpoint control (71) has also been suggested by the observation that purified recombinant GADD45a inhibits the histone H1 kinase activity associated with the cyclin B–Cdc2 complex by inducing the dissociation of this complex, which is required for G_2 transition (74). A central region of human GADD45a (amino acids 65–84) has been shown to mediate its interaction with Cdc2 (also known as CDK1) and to be required for inhibition of the kinase activity of Cdc2. FOXO directly binds and activates the promoter of the GADD45a gene and increases the amount of GADD45a protein (20, 66). Further evidence that FOXO-induced G_2 arrest is mediated by GADD45a was provided by the observation that such arrest is partially compromised in GADD45a-deficient mouse embryonic fibroblasts (66). GADD45a is also a stress-inducible protein, and its induction by FOXO is implicated in the cellular stress response (see below).

OXIDATIVE STRESS AND FOXO

An absence of Akt signaling in *C. elegans* results in activation of the FOXO homologue DAF-16 and in dauer formation, a phenotype that is characterized by increased resistance to oxidative stress (27, 49, 50). The stress resistance phenotype is dependent on DAF-16, implicating this transcription factor in the regulation of genes related to stress resistance (30, 65). Similarly, mammalian FOXO plays a role in cellular resistance to oxidative stress. In quiescent cells that lack Akt activity, FOXO localizes to the nucleus and induces the expression of manganese superoxide dismutase, an antioxidant enzyme that confers resistance to oxidative stress (35). FOXO3a also upregulates the expression of sterol carrier protein x (SCPx) and SCP2 (13). SCPx is a thiolase that contributes to the breakdown of branched chain fatty acids and to the biosynthesis of bile acids, whereas SCP2 has been shown to protect bound fatty acids against oxidative damage induced by the combination of hydrogen peroxide (H_2O_2) and Cu^{2+} (13).

REGULATION OF FOXO IN RESPONSE TO OXIDATIVE STRESS

Among various genes that are regulated by FOXO, that for GADD45a is induced by a variety of stressors, including ionizing radiation, UV, and reactive oxygen species such as H_2O_2, suggesting that FOXO might also be activated by cellular stress. DAF-16 translocates from the cytoplasm to the nucleus in response to certain types of oxidative stress in *C. elegans* (24). Similarly, oxidative stress caused by H_2O_2, menadione, or heat shock triggers the relocalization of FOXO from the cytoplasm to the nucleus in mammalian fibroblasts exposed to growth factors (9, 33) (Fig. 4). The apparent nuclear accumulation of FOXO in the nucleus of cells not exposed to growth factors is not further increased by stimulation of these cells with H_2O_2. FOXO3a is phosphorylated on eight serine or threonine residues, not including those residues targeted by Akt, in response to oxidative stress, although the kinases responsible for such phosphorylation remain to be identified (9). It is possible that some of these phosphorylation events triggered by stress interfere with the interaction between FOXO and 14-3-3, thereby inducing nuclear accumulation of FOXO. Alternatively, in this regard, c-Jun NH_2-terminal kinase (JNK) phosphorylates 14-3-3 and thereby induces dissociation of its target protein Bax (67). JNK is a member of a group of mitogen-activated protein kinases, known as stress-activated protein kinases, that are activated by oxidative stress (15). It is therefore possible that 14-3-3 is phosphorylated by JNK that has been activated by oxidative stress and that its phosphorylation promotes its dissociation from FOXO, thereby allowing translocation of FOXO to the nucleus.

In addition to inducing its nuclear translocation, oxidative stress promotes the interaction of FOXO with protein acetylases, including p300 [or the related protein CREB-binding protein (CBP)] and p300/CBP–associated factor (PCAF), and its consequent acetylation at several lysine residues (9, 19, 33, 40, 44, 48, 68). Human FOXO4 is acetylated by CBP at lysines

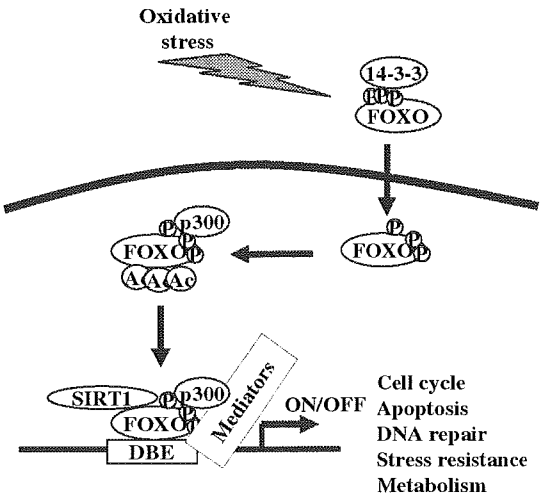

FIG. 4. Relocalization and activation of FOXO in response to oxidative stress. Oxidative stress induces the phosphorylation of FOXO by unidentified kinases and its consequent translocation to the nucleus. The transcriptional coactivator p300 (or CBP) interacts with FOXO and catalyzes its acetylation on several lysine residues, resulting in inhibition of its transactivation activity. The deacetylase SIRT1 also binds to and deacetylates FOXO, thereby reversing the inhibitory effect of p300 on FOXO activity. The effects of acetylation and deacetylation of FOXO, however, appear to be promoter-specific; whereas SIRT1 enhances the FOXO-mediated expression of genes that contribute to cell-cycle regulation or the stress response, it suppresses that of genes whose products participate in apoptosis.

186, 189, and 408 *in vitro* (19). An additional lysine residue of FOXO4, lysine 237, is also acetylated by p300 and CBP *in vivo* (33). The acetylation of FOXO4 by p300 (or CBP) inhibited its activation of a promoter containing multiple copies of the FOXO response element linked to a reporter gene, as well as of $p27^{Kip1}$ expression, indicating that acetylation inhibits the transactivation activity of FOXO4 directly (19, 33). Human FOXO3a is also acetylated on five lysine residues (lysines 242, 259, 271, 290, and 569) in response to oxidative stress (9).

A physiological interaction of FOXO with SIRT1, an NAD^+-dependent deacetylase and the closest homologue of yeast SIR2 among the seven members of the mammalian sirtuin family (9, 33, 44, 68), has also been demonstrated. The binding of SIRT1 to FOXO is accompanied by deacetylation of the latter in an NAD^+-dependent manner. Deacetylation of transcriptional complexes including transcription factors and histones has been traditionally associated with repression of target gene expression. However, deacetylation of histones and unidentified molecules by the yeast histone deacetylase Rpd3 was recently shown to be required for gene expression in response to stress, including oxidative stress (16). The deacetylation of FOXO by SIRT1 also appears to reverse the inhibitory effect of acetylation on its transactivation activity. Depletion of endogenous SIRT1 in SaoS2 cells (which lack p53) by RNA interference thus resulted in impairment of FOXO-mediated GADD45a expression induced by oxidative stress (33). However, the effect of FOXO acetylation–deacetylation on the transcription of target genes is not quite so straightforward. SIRT1 has thus been shown to suppress the FOXO-mediated expression of genes, such as those for Bim and Fas ligand, that contribute to the apoptotic response, suggesting that the regulation of FOXO activity by acetylation–deacetylation is promoter-specific (9).

CONCLUSION

The FOXO family of proteins regulates various biological activities, including cell-cycle progression, the cellular response to oxidative stress, DNA repair, and apoptosis. The activity of FOXO proteins is regulated by phosphorylation by multiple protein kinases, as well as by acetylation and deacetylation. Phosphorylation of three highly conserved residues of FOXO by the PI3K-Akt signaling pathway results in the nuclear exclusion of FOXO mediated by interactions with 14-3-3, the Ran GTPase, and Crm1 and in the consequent inhibition of target gene transcription. Deregulation of the PI3K-Akt signaling pathway is implicated in tumorigenesis. The tumor suppressor PTEN regulates FOXO through the PI3K-Akt signaling pathway (47). In addition, like the tumor suppressor p53, FOXO is activated by oxidative stress and other stressors and induces the expression of genes that contribute to cell-cycle arrest, suggesting that FOXO also functions as a tumor suppressor.

ACKNOWLEDGMENTS

We thank members of the Department of Geriatric Research for stimulating discussions. Yoko Furukawa-Hibi is a research fellow of the Japan Society for the Promotion of Sciences. Research in the author's laboratory was supported by a Grant-in-Aid for Scientific Research from the Ministry of Education, Culture, Sports, Sciences and Technology of Japan.

ABBREVIATIONS

CBP, CREB-binding protein; CDK, cyclin-dependent kinase; CK1, casein kinase 1; CKI, CDK inhibitor; DYRK1A, dual-specificity tyrosine-phosphorylated and regulated kinase 1A; FOXO, forkhead member of the class O; GADD45a, growth arrest– and DNA damage–inducible protein a of 45 kDa; H_2O_2, hydrogen peroxide; IGF-1, insulin-like growth factor–1; JNK, c-Jun NH_2-terminal kinase; NES, nuclear export sequence; NLS, nuclear localization sequence; PDK1, 3'-phosphoinositide–dependent kinase 1; PI3K, phosphatidylinositol 3-kinase; PIP_3, phosphatidylinositol 3,4,5-trisphosphate; PTEN, phosphatase and tensin homologue on chromosome 10; SCP, sterol carrier protein; SGK, serum- and glucocorticoid-induced kinase; UV, ultraviolet light.

REFERENCES

1. Anderson MJ, Viars CS, Czekay S, Cavenee WK, and Arden KC. Cloning and characterization of three human forkhead genes that comprise an FKHR-like gene subfamily. *Genomics* 47: 187–199, 1998.
2. Bennin DA, Don AS, Brake T, McKenzie JL, Rosenbaum H, Ortiz L, DePaoli-Roach AA, and Horne MC. Cyclin G2 associates with protein phosphatase 2A catalytic and regulatory B' subunits in active complexes and induces nuclear aberrations and a G_1/S phase cell cycle arrest. *J Biol Chem* 277: 27449–27467, 2002.
3. Biggs WH 3rd, Meisenhelder J, Hunter T, Cavenee WK, and Arden KC. Protein kinase B/Akt-mediated phosphorylation promotes nuclear exclusion of the winged helix transcription factor FKHR1. *Proc Natl Acad Sci U S A* 96: 7421–7426, 1999.
4. Borkhardt A, Repp R, Haas OA, Leis T, Harbott J, Kreuder J, Hammermann J, Henn T, and Lampert F. Cloning and characterization of AFX, the gene that fuses to MLL in acute leukemias with a t(X;11)(q13;q23). *Oncogene* 14: 195–202, 1997.
5. Brownawell AM, Kops GJ, Macara IG, and Burgering BM. Inhibition of nuclear import by protein kinase B (Akt) regulates the subcellular distribution and activity of the forkhead transcription factor AFX. *Mol Cell Biol* 21: 3534–3546, 2001.
6. Brunet A, Bonni A, Zigmond MJ, Lin MZ, Juo P, Hu LS, Anderson MJ, Arden KC, Blenis J, and Greenberg ME. Akt promotes cell survival by phosphorylating and inhibiting a Forkhead transcription factor. *Cell* 96: 857–868, 1999.
7. Brunet A, Park J, Tran H, Hu LS, Hemmings BA, and Greenberg ME. Protein kinase SGK mediates survival signals by phosphorylating the forkhead transcription factor FKHRL1 (FOXO3a). *Mol Cell Biol* 21: 952–965, 2001.

8. Brunet A, Kanai F, Stehn J, Xu J, Sarbassova D, Frangioni JV, Dalal SN, DeCaprio JA, Greenberg ME, and Yaffe MB. 14-3-3 transits to the nucleus and participates in dynamic nucleocytoplasmic transport. *J Cell Biol* 156: 817–828, 2002.
9. Brunet A, Sweeney LB, Sturgill JF, Chua KF, Greer PL, Lin,Y, Tran H, Ross SE, Mostoslavsky R, Cohen HY, Hu LS, Cheng HL, Jedrychowski MP, Gygi SP, Sinclair DA, Alt FW, and Greenberg ME. Stress-dependent regulation of FOXO transcription factors by the SIRT1 deacetylase. *Science* 303: 2011–2015, 2004.
10. Buse P, Tran SH, Luther E, Phu PT, Aponte GW, and Firestone GL. Cell cycle and hormonal control of nuclear-cytoplasmic localization of the serum- and glucocorticoid-inducible protein kinase, Sgk, in mammary tumor cells. A novel convergence point of anti-proliferative and proliferative cell signaling pathways. *J Biol Chem* 274: 7253–7263, 1999.
11. Cantley LC. The phosphoinositide 3-kinase pathway. *Science* 296: 1655–1657, 2002.
12. Cantley LC and Neel BG. New insights into tumor suppression: PTEN suppresses tumor formation by restraining the phosphoinositide 3-kinase/Akt pathway. *Proc Natl Acad Sci U S A* 96: 4240–4245, 1999.
13. Dansen TB, Kops GJ, Denis S, Jelluma N, Wanders RJ, Bos JL, Burgering BM, and Wirtz KW. Regulation of sterol carrier protein gene expression by the Forkhead transcription factor FOXO3a. *J Lipid Res* 45: 81–88, 2004.
14. Datta SR, Brunet A, and Greenberg ME. Cellular survival: a play in three Akts. *Genes Dev* 13: 2905–2927, 1999.
15. Davis RJ. Signal transduction by the JNK group of MAP kinases. *Cell* 103: 239–252, 2000.
16. De Nadal E, Zapater M, Alepuz PM, Sumoy L, Mas G, and Posas F. The MAPK Hog1 recruits Rpd3 histone deacetylase to activate osmoresponsive genes. *Nature* 427: 370–374, 2004.
17. De Ruiter ND, Burgering BM, and Bos JL. Regulation of the Forkhead transcription factor AFX by Ral-dependent phosphorylation of threonines 447 and 451. *Mol Cell Biol* 21: 8225–8235, 2001.
18. Friedman DB and Johnson TE. A mutation in the *age-1* gene in *Caenorhabditis elegans* lengthens life and reduces hermaphrodite fertility. *Genetics* 118: 75–86, 1998.
19. Fukuoka M, Daitoku H, Hatta M, Matsuzaki H, Umemura S, and Fukamizu A. Negative regulation of forkhead transcription factor AFX (Foxo4) by CBP-induced acetylation. *Int J Mol Med* 12: 503–508, 2003.
20. Furukawa-Hibi Y, Yoshida-Araki K, Ohta T, Ikeda K, and Motoyama N. FOXO forkhead transcription factors induce G_2-M checkpoint in response to oxidative stress. *J Biol Chem* 277: 26729–26732, 2002.
21. Furuyama T, Nakazawa T, Nakano I, and Mori N. Identification of the differential distribution patterns of mRNAs and consensus binding sequences for mouse DAF-16 homologues. *Biochem J* 349: 629–634, 2000.
22. Galili N, Davis RJ, Fredericks WJ, Mukhopadhyay S, Rauscher FJ 3rd, Emanuel BS, Rovera G, and Barr FG. Fusion of a fork head domain gene to PAX3 in the solid tumour alveolar rhabdomyosarcoma. *Nat Genet* 5: 230–235, 1993.
23. Grana X, Garriga J, and Mayol X. Role of the retinoblastoma protein family, pRB, p107 and p130 in the negative control of cell growth. *Oncogene* 17: 3365–3383, 1998.
24. Henderson ST and Johnson TE. *daf-16* integrates developmental and environmental inputs to mediate aging in the nematode *Caenorhabditis elegans*. *Curr Biol* 11: 1975–1980, 2001.
25. Hertweck M, Gobel C, and Baumeister R. *C. elegans* SGK-1 is the critical component in the Akt/PKB kinase complex to control stress response and life span. *Dev Cell* 6: 577–588, 2004.
26. Hillion J, Le Coniat M, Jonveaux P, Berger R, and Bernard OA. AF6q21, a novel partner of the MLL gene in t(6;11)(q21;q23), defines a forkhead transcriptional factor subfamily. *Blood* 90: 3714–3719, 1997.
27. Honda Y and Honda S. The *daf-2* gene network for longevity regulates oxidative stress resistance and Mn-superoxide dismutase gene expression in *Caenorhabditis elegans*. *FASEB J* 13: 1385–1393, 1999.
28. Horne MC, Donaldson KL, Goolsby GL, Tran D, Mulheisen M, Hell JW, and Wahl AF. Cyclin G2 is up-regulated during growth inhibition and B cell antigen receptor-mediated cell cycle arrest. *J Biol Chem* 272: 12650–12661, 1997.
29. Hunter T and Pines J. Cyclins and cancer. II: Cyclin D and CDK inhibitors come of age. *Cell* 79: 573–582, 1994.
30. Kenyon C, Chang J, Gensch E, Rudner A, and Tabtiang R. A *C. elegans* mutant that lives twice as long as wild type. *Nature* 366: 461–464, 1993.
31. Klippel A, Escobedo MA, Wachowicz MS, Apell G, Brown TW, Giedlin MA, Kavanaugh WM, and Williams LT. Activation of phosphatidylinositol 3-kinase is sufficient for cell cycle entry and promotes cellular changes characteristic of oncogenic transformation. *Mol Cell Biol* 18: 5699–5711, 1998.
32. Kobayashi T and Cohen P. Activation of serum- and glucocorticoid-regulated protein kinase by agonists that activate phosphatidylinositide 3-kinase is mediated by 3-phosphoinositide-dependent protein kinase-1 (PDK1) and PDK2. *Biochem J* 339 (Pt 2): 319–328, 1999.
33. Kobayashi Y Furukawa-Hibi Y, Chen C, Horio Y, Ikeda K, and Motoyama N. SIRT1 is critical regulator of FOXO-mediated transcription in response to oxidative stress. (Submitted.)
34. Kops GJ, de Ruiter ND, De Vries-Smits AM, Powell DR, Bos JL, and Burgering BM. Direct control of the Forkhead transcription factor AFX by protein kinase B. *Nature* 398: 630–634, 1999.
35. Kops GJ, Dansen TB, Polderman PE, Saarloos I, Wirtz KW, Coffer PJ, Huang TT, Bos JL, Medema RH, and Burgering BM. Forkhead transcription factor FOXO3a protects quiescent cells from oxidative stress. *Nature* 419: 316–321, 2002.
36. Kops GJ, Medema RH, Glassford J, Essers MA, Dijkers PF, Coffer PJ, Lam EW, and Burgering BM. Control of cell cycle exit and entry by protein kinase B-regulated forkhead transcription factors. *Mol Cell Biol* 22: 2025–2036, 2002.
37. Larsen PL. Aging and resistance to oxidative damage in *Caenorhabditis elegans*. *Proc Natl Acad Sci U S A* 90: 8905–8909, 1993.

38. Lin K, Dorman JB, Rodan A, and Kenyon C. *daf-16*: an HNF-3/forkhead family member that can function to double the life-span of *Caenorhabditis elegans*. *Science* 278: 1319–1322, 1997.
39. Lithgow GJ, White TM, Melov S, and Johnson TE. Thermotolerance and extended life-span conferred by single-gene mutations and induced by thermal stress. *Proc Natl Acad Sci U S A* 92: 7540–7544, 1995.
40. Mahmud DL, G-Amlak M, Deb DK, Platanias LC, Uddin S, and Wickrema A. Phosphorylation of forkhead transcription factors by erythropoietin and stem cell factor prevents acetylation and their interaction with coactivator p300 in erythroid progenitor cells. *Oncogene* 21: 1556–1562, 2002.
41. Martinez-Gac L, Marques M, Garcia Z, Campanero MR, and Carrera AC. Control of cyclin G2 mRNA expression by forkhead transcription factors: novel mechanism for cell cycle control by phosphoinositide 3-kinase and forkhead. *Mol Cell Biol* 24: 2181–2189, 2004.
42. Medema RH, Kops GJ, Bos JL, and Burgering BM. AFX-like Forkhead transcription factors mediate cell-cycle regulation by Ras and PKB through $p27^{kip1}$. *Nature* 404: 782–787, 2000.
43. Motoyama N and Naka K. DNA damage tumor suppressor genes and genomic instability. *Curr Opin Genet Dev* 14: 11–16, 2004.
44. Motta MC, Divecha N, Lemieux M, Kamel C, Chen D, Gu W, Bultsma Y, McBurney M, and Guarente L. Mammalian SIRT1 represses forkhead transcription factors. *Cell* 116: 551–563, 2004.
45. Murakami S and Johnson TE. A genetic pathway conferring life extension and resistance to UV stress in *Caenorhabditis elegans*. *Genetics* 143: 1207–1218, 1996.
46. Murphy CT, McCarroll SA, Bargmann CI, Fraser A, Kamath RS, Ahringer J, Li H, and Kenyon C. Genes that act downstream of DAF-16 to influence the lifespan of *Caenorhabditis elegans*. *Nature* 424: 277–283, 2003.
47. Nakamura N, Ramaswamy S, Vazquez F, Signoretti S, Loda M, and Sellers WR. Forkhead transcription factors are critical effectors of cell death and cell cycle arrest downstream of PTEN. *Mol Cell Biol* 20: 8969–8982, 2000.
48. Nasrin N, Ogg S, Cahill CM, Biggs W, Nui S, Dore J, Calvo D, Shi Y, Ruvkun G, and Alexander-Bridges MC. DAF-16 recruits the CREB-binding protein coactivator complex to the insulin-like growth factor binding protein 1 promoter in HepG2 cells. *Proc Natl Acad Sci U S A* 97: 10412–10417, 2000.
49. Ogg S, Paradis S, Gottlieb S, Patterson GI, Lee L, Tissenbaum HA, and Ruvkun G. The Fork head transcription factor DAF-16 transduces insulin-like metabolic and longevity signals in *C. elegans*. *Nature* 389: 994–999, 1997.
50. Paradis S, and Ruvkun G. *Caenorhabditis elegans* Akt/PKB transduces insulin receptor-like signals from AGE-1 PI3 kinase to the DAF-16 transcription factor. *Genes Dev* 12: 2488–2498, 1998.
51. Park J, Leong ML, Buse P, Maiyar AC, Firestone GL, and Hemmings BA. Serum and glucocorticoid-inducible kinase (SGK) is a target of the PI 3-kinase-stimulated signaling pathway. *EMBO J* 18: 3024–3033, 1999.
52. Ramaswamy S, Nakamura N, Sansal I, Bergeron L, and Sellers WR. A novel mechanism of gene regulation and tumor suppression by the transcription factor FKHR. *Cancer Cell* 2: 81–91, 2002.
53. Rena G, Guo S, Cichy SC, Unterman TG, and Cohen P. Phosphorylation of the transcription factor forkhead family member FKHR by protein kinase B. *J Biol Chem* 274: 17179–17183, 1999.
54. Rena G, Woods YL, Prescott AR, Peggie M, Unterman TG, Williams MR, and Cohen P. Two novel phosphorylation sites on FKHR that are critical for its nuclear exclusion. *EMBO J* 21: 2263–2271, 2002.
55. Reynisdottir I, Polyak K, Iavarone A, and Massague J. Kip/Cip and Ink4 Cdk inhibitors cooperate to induce cell cycle arrest in response to TGF-beta. *Genes Dev* 9: 1831–1845, 1995.
56. Schmidt M, Fernandez de Mattos S, van der Horst A, Klompmaker R, Kops GJ, Lam EW, Burgering BM, and Medema RH. Cell cycle inhibition by FoxO forkhead transcription factors involves downregulation of cyclin D. *Mol Cell Biol* 22: 7842–7852, 2002.
57. Sherr CJ. G_1 phase progression: cycling on cue. *Cell* 79: 551–555, 1994.
58. Sherr CJ and Roberts JM. Inhibitors of mammalian G1 cyclin-dependent kinases. *Genes Dev* 9: 1149–1163, 1995.
59. Sherr CJ and Roberts JM. CDK inhibitors: positive and negative regulators of G_1-phase progression. *Genes Dev* 13: 1501–1512, 1999.
60. Smith EJ, Leone G, DeGregori J, Jakoi L, and Nevins JR. The accumulation of an E2F-p130 transcriptional repressor distinguishes a G_0 cell state from a G_1 cell state. *Mol Cell Biol* 16: 6965–6976, 1996.
61. Stahl M, Dijkers PF, Kops GJ, Lens SM, Coffer PJ, Burgering BM, and Medema RH. The forkhead transcription factor FoxO regulates transcription of $p27^{Kip1}$ and Bim in response to IL-2. *J Immunol* 168: 5024–5031, 2002.
62. Takaishi H, Konishi H, Matsuzaki H, Ono Y, Shirai Y, Saito N, Kitamura T, Ogawa W, Kasuga M, Kikkawa U, and Nishizuka Y. Regulation of nuclear translocation of forkhead transcription factor AFX by protein kinase B. *Proc Natl Acad Sci U S A* 96: 11836–11841, 1999.
63. Tanaka M, Kirito K, Kashii Y, Uchida M, Watanabe T, Endo H, Endoh T, Sawada K, Ozawa K, and Komatsu N. Forkhead family transcription factor FKHRL1 is expressed in human megakaryocytes. Regulation of cell cycling as a downstream molecule of thrombopoietin signaling. *J Biol Chem* 276: 15082–15089, 2001.
64. Tang ED, Nunez G, Barr FG, and Guan KL. Negative regulation of the forkhead transcription factor FKHR by Akt. *J Biol Chem* 274: 16741–16746, 1999.
65. Tissenbaum HA and Ruvkun G. An insulin-like signaling pathway affects both longevity and reproduction in *Caenorhabditis elegans*. *Genetics* 148: 703–717, 1998.
66. Tran H, Brunet A, Grenier JM, Datta SR, Fornace AJ Jr, DiStefano PS, Chiang LW, and Greenberg ME. DNA repair pathway stimulated by the forkhead transcription factor FOXO3a through the Gadd45 protein. *Science* 296: 530–534, 2002.
67. Tsuruta F, Sunayama J, Mori Y, Hattori S, Shimizu S, Tsujimoto Y, Yoshioka K, Masuyama N, and Gotoh Y. JNK

promotes Bax translocation to mitochondria through phosphorylation of 14-3-3 proteins. *EMBO J* 23: 1889–1899, 2004.
68. Van Der Horst A, Tertoolen LG, De Vries-Smits LM, Frye RA, Medema RH, and Burgering BM. FOXO4 is acetylated upon peroxide stress and deacetylated by the longevity protein hSir2^{SIRT1}. *J Biol Chem* 279: 28873–28879, 2004.
69. Vanfleteren JR. Oxidative stress and ageing in *Caenorhabditis elegans*. *Biochem J* 292 (Pt 2): 605–608, 1993.
70. Vivanco I and Sawyers CL. The phosphatidylinositol 3-kinase Akt pathway in human cancer. *Nat Rev Cancer* 2: 489–501, 2002.
71. Wang XW, Zhan Q, Coursen JD, Khan MA, Kontny HU, Yu, L, Hollander MC, O'Connor PM, Fornace AJ Jr, and Harris CC. GADD45 induction of a G_2/M cell cycle checkpoint. *Proc Natl Acad Sci U S A* 96: 3706–3711, 1999.
72. Woods YL, Rena G, Morrice N, Barthel A, Becker W, Guo S, Unterman TG, and Cohen P. The kinase DYRK1A phosphorylates the transcription factor FKHR at Ser329 in vitro, a novel in vivo phosphorylation site. *Biochem J* 355: 597–607, 2001.
73. Yaffe MB, Rittinger K, Volinia S, Caron PR, Aitken A, Leffers H, Gamblin SJ, Smerdon SJ, and Cantley LC. The structural basis for 14-3-3:phosphopeptide binding specificity. *Cell* 91: 961–971, 1997.
74. Zha Q, Antinore MJ, Wang XW, Carrier F, Smith ML, Harris CC, and Fornace AJ Jr. Association with Cdc2 and inhibition of Cdc2/cyclin B1 kinase activity by the p53-regulated protein Gadd45. *Oncogene* 18: 2892–2900, 1999.
75. Zhou BB and Elledge SJ. The DNA damage response: putting checkpoints in perspective. *Nature* 408: 433–439, 2000.

Address reprint requests to:
Noboru Motoyama, Ph.D.
Department of Geriatric Research
National Institute for Longevity Sciences
National Center for Geriatrics and Gerontology
36-3 Gengo
Morioka, Obu
Aichi 474-8522, Japan

E-mail: motoyama@nils.go.jp

Received for publication September 24, 2004; accepted November 30, 2004.

SIRT1 is critical regulator of FOXO-mediated transcription in response to oxidative stress

YOSUKE KOBAYASHI[1,3*], YOKO FURUKAWA-HIBI[1*], CHEN CHEN[1*], YOSHIYUKI HORIO[4], KENICHI ISOBE[2,3], KYOJI IKEDA[1] and NOBORU MOTOYAMA[1]

Departments of [1]Geriatric Research and [2]Mechanism of Aging, National Institute for Longevity Sciences, National Center for Geriatrics and Gerontology, Obu, Aichi 474-8522; [3]Department of Aging Research, Nagaya University Graduate School of Medicine, Nagoya, Aichi 466-8550; [4]Department of Pharmacology, Sapporo Medical University, School of Medicine, Sapporo, Hokkaido 060-8556, Japan

Received March 3, 2005; Accepted April 18, 2005

Abstract. Forkhead transcription factor, DAF-16, regulates genes that contribute both to longevity and resistance to various stresses in *C. elegans*. We and others have reported that members of the FOXO, mammalian homologs of DAF-16, also regulate genes related to stress resistance, such as GADD45. The NAD-dependent protein deacetylase, SIR2, is required for life span extension in yeast induced by caloric restriction, which also increases longevity in a wide variety of other organisms, including mammals. Sir2.1, a homolog of yeast SIR2, also extends life span by acting in a DAF-16 signaling pathway in *C. elegans*. We demonstrate that mammalian SIRT1 (Sir2α) physiologically interacts with FOXO. Acetylation of FOXO4, by the transcriptional coactivator p300, counteracted transcriptional activation of FOXO4 by p300. In contrast, mammalian SIRT1 was found to bind to FOXO4, catalyze its deacetylation in an NAD-dependent manner, and thereby increase its transactivation activity. The activity of FOXO4 is suppressed or enhanced by SIRT1 inhibitor, nicotinamide, or its activator, resveratrol, respectively. In response to oxidative stress, FOXO accumulates within the nucleus and induces GADD45 expression. FOXO-mediated GADD45 induction is markedly impaired in the cell, which depleted SIRT1 expression by RNA-interference. These results indicate that mammalian SIRT1 plays a pivotal role for FOXO function via NAD-dependent deacetylation in response to oxidative stress, and thereby may contribute to cellular stress resistance and longevity.

Correspondence to: Dr Noboru Motoyama, Department of Geriatric Research, National Institute for Longevity Sciences, National Center for Geriatrics and Gerontology, 36-3 Gengo, Morioka, Obu, Aichi 474-8522, Japan
E-mail: motoyama@nils.go.jp

*Contributed equally

Key words: acetylation, deacetylation, FOXO, GADD45, oxidative stress, SIRT1

Introduction

Certain single-gene mutations, such as *daf-2* and *age-1*, extend life span and increase resistance to a variety of environmental effects, including oxidative stress and ultraviolet radiation in the nematode *C. elegans* (1,2). The longevity and stress-resistant phenotypes are dependent on the forkhead transcription factor, DAF-16, which acts downstream of DAF-2/AGE-1 signaling, implicating this protein in the regulation of genes related to stress resistance (3,4). This signal cascade is conserved in mammals. The insulin/insulin-like growth factor (IGF) receptor (DAF-2) activates protein kinase B (PKB; also known as c-Akt) through the phosphatidylinositol-3-OH kinase (PI-3K), which phosphorylates and inhibits mammalian FOXO family proteins by stimulating their nuclear exclusion (5,6). Members of the mammalian FOXO family, including FOXO3 and FOXO4, also contribute to stress resistance by regulating genes, such as those for GADD45 (7,8) and MnSOD (9), suggesting that FOXO also may participate in the regulation of life span in mammalian cells, such as in invertebrates.

Yeast SIR2 mediates genomic silencing at telomeres, mating-type loci, and ribosomal DNA repeats, as well as regulating aging. SIR2 possesses an NAD-dependent histone deacetylase activity that is required for both chromatin silencing and life span extension (10-12). SIRT1 (Sir2α), a mammalian homolog of yeast SIR2, functions as an NAD-dependent deacetylase for transcription factors such as p53, as well as for histone (13-15). The extension of life span in *C. elegans* induced by overexpression of Sir2.1, also a homolog of yeast SIR2, is thought to result from the action of this protein in a DAF-2-AGE-1-DAF-16 signaling pathway (16). These observations prompted us to examine whether mammalian SIRT1 directly regulates FOXO function.

In the present study, we have discovered that oxidative stress, FOXOs and SIRT1 are linked. Our results indicate that SIRT1 plays a key role in the FOXO-mediated gene expression in response to oxidative stress.

Materials and methods

Plasmids. Mouse SIRT1 and SIRT3 cDNAs were described previously (17). The cDNA for SIRT1-HY, in which His^{355} of SIRT1 is replaced by tyrosine, was generated with the use of a QuickChange Mutagenesis kit (Invitrogen). The expression vector for HA-p300 and HA-CBP were kindly provided by R. Eckner, M. Ikeda and A. Fukamizu. The pCXN2-FLAG-FOXO4-WT, pCXN2-FLAG-FOXO4-TM, and pG45-817 plasmids were described previously (8). The pcDNA3.1-myc-FOXO4-TM vector was generated by subcloning the FOXO4 cDNA fragment into pcDNA3.1-myc-his. The several Myc epitope-tagged mutants of FOXO4-TM, in which lysine (K) residues were replaced by arginine (R), were generated with the use of a QuickChange Mutagenesis kit. Retroviral vectors, pMX-puro and pMX-neo, were provided by T. Kitamura.

Cell lines, transfection and infection. The 293T, COS-7, HCT-116, Saos2, MEF and NIH 3T3 cells were cultured in Dulbecco's modified Eagle's medium supplemented with 10% fetal bovine serum. Jurkat cells were maintained in RPMI medium supplemented with 10% fetal bovine serum. Transfection of cells with the various expression plasmids was performed with the use of the FuGENE6 reagent (Roche). Retroviruses expressing FLAG-FOXO4, FLAG-FOXO4-TM, FLAG-SIRT1 and FLAG-SIRT1-HY were produced by transfection into PLAT-E packaging cells (provided by T. Kitamura), and infected NIH3T3 or MEFs were then selected in medium containing 2 μg/ml puromycin or 1.2 μg/ml neomycin.

Immunoprecipitation and immunoblot analysis. Cells were lysed and subjected to immunoprecipitation as described (18). For the detection of acetylated FOXO proteins, cells were lysed in a lysis buffer containing 50 μM trichostatin A and 100 mM nicotinamide (Sigma). The primary antibodies used in this study included those for FLAG (M2 and M5, Sigma), Myc and HA (Medical Biological Laboratory), His6 (Covance), SIRT1, p27, FOXO3 and FOXO4 (Santa Cruz Biotechnology), acetyl lysine (Cell Signaling and UP State), and α-tubulin (Sigma). Immune complexes were developed with the ECL Plus system (Amersham).

In vitro deacetylation assay. *In vitro* deacetylation assay was performed as reported by North *et al* (19). Briefly, 293T cells were transfected with pcDNA3, pcDNA3-FLAG- SIRT1, or pcDNA3-FLAG- SIRT1-HY expression plasmids, then subjected to immunoprecipitation with antibodies for FLAG and protein G-coupled magnetic beads (Dyna beads); the resulting precipitates were used for deacetylation reactions. Acetylated FOXO4 and FOXO3a were prepared by co-transfection of 293T cells with vectors for Myc-FOXO4-TM or FLAG-FOXO3a-TM and HA-p300. Whole cell lysates containing acetylated FOXO4 or FOXO3a were then incubated for 2 h at 30˚C with the immunoprecipitated SIRT1 in HDAC buffer (50 mM Tris-HCl pH 9.0, 4 mM $MgCl_2$, and 0.2 mM dithiothreitol) in the absence or presence of 1 mM NAD, 0.5 μM trichostatin A, or 5 mM nicotinamide. Reaction mixtures were immunoprecipitated with antibodies to Myc for FOXO4, or FLAG for FOXO3a, then analyzed by immunoblot analysis with antibodies for acetyl lysine.

Luciferase assay. Cells were transfected with pGL-6xDBE or pG45-817 reporter plasmids together with phRG-TK and expression vectors for FOXO4 or SIRT1. After incubation in the absence or presence of resveratrol (Biomol) or nicotinamide, cells were lysed and assayed for luciferase activities with the Dual-Luciferase Reporter Assay System (Promega); transfection efficiency was normalized by *Renilla* luciferase activity derived from phRG-TK.

RNA interference. The 21-bp siRNA duplexes included a 2-base overhang. The sequence of the pan-FOXO and SIRT1 siRNA were 5'-GGAUAAGGGCGACAGCAACTT and 5'-CUUGUACGACGAAGACGACTT, respectively. The GFP siRNA was obtained from Qiagen. Cells were transfected with the siRNA duplexes with the use of oligofectamine (Invitrogen).

Results

Acetylation of FOXO4 by p300 decreases its transcriptional activity. Both FOXO3 and FOXO1 are acetylated by p300 *in vitro*, but the biological significance of this modification is not clear (20). We first examined whether mouse FOXO4 and FOXO3 is acetylated by p300 *in vivo*. We transfected 293T cells with expression vectors for hemagglutinin epitope (HA)-tagged p300, and FLAG epitope-tagged FOXO4-TM and FOXO3-TM, a mouse FOXO4 and FOXO3 mutant, in which the three sites for phosphorylation by Akt have been replaced by alanine, which is both constitutively active and restricted to the nucleus. Immunoprecipitation and immunoblot analysis of the transfected cells revealed that FOXO4-TM and FOXO3-TM were acetylated in cells that overexpressed p300, but not in those that did not (Fig. 1A and B). Although it has been recently reported that FOXO4 are acetylated by coactivator CBP on lysine (K) 186, 189 and 408 *in vitro* (21), FOXO4-TM-3KR (K186, 189 and 408 are replaced by arginine (R)) were still acetylated by p300. To determine the site of acetylation in FOXO4, we generated several Myc epitope-tagged mutants of FOXO4-TM in which lysine residues, in addition to K186, 189 and 408, were replaced by arginine, and tested whether the mutant proteins were acetylated in 293T cells coexpressing HA-p300. Of the various mutants tested, only the K237 substitution mutant of FOXO4-TM-3KR (FOXO4-TM-4KR) resulted in markedly reduced acetylation by p300 *in vivo*, suggesting that FOXO4 is acetylated by p300 on K186, 189, 237 and 408 (Fig. 1C).

To clarify the functional consequence of FOXO4 acetylation, we subjected COS-7 cells to transient transfection, both with a luciferase reporter plasmid (pGL-6xDBE) that contains six tandem repeats of the DNA binding consensus element for FOXO proteins, and an expression vector for FOXO4-TM or FOXO4-TM-4KR, in the absence or presence of a p300 expression plasmid. Coexpression of p300 increased the transactivation activity of FOXO4-TM or FOXO4-TM-4KR. However, the effect of p300 on the activity of FOXO4-TM-4KR was more pronounced than that on FOXO4-TM activity with comparable expression of p300 (Fig. 1D). Thus, the

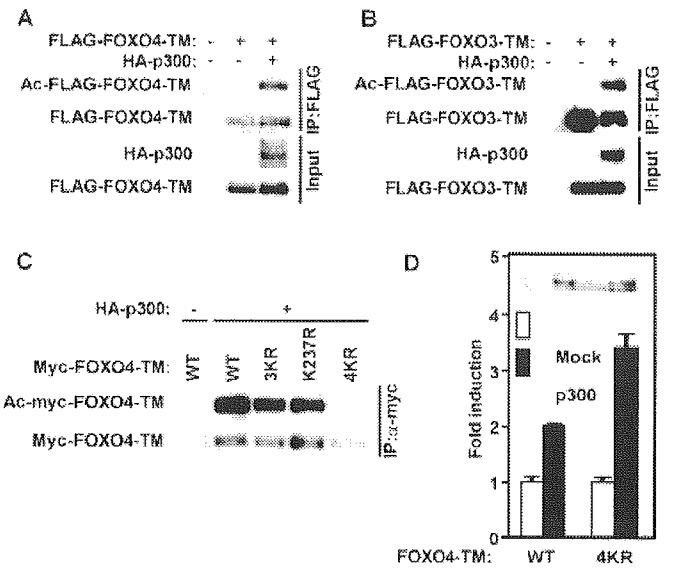

Figure 1. Acetylation of FOXO protein and inhibition of its transactivation activity by p300. (A and B) The 293T cells were transfected with expression vectors for FLAG-tagged FOXO4-TM, FLAG-FOXO3-TM, and HA-tagged p300, as indicated, then subjected to immunoprecipitation (IP) with antibodies for FLAG. The resulting precipitates were subjected to immunoblot analysis with antibodies for HA (HA-p300), FLAG (FLAG-FOXO4-TM), acetyl lysine, or α-tubulin (control). Cell lysates (input) were also subjected directly to immunoblot analysis with the same antibodies. (C) The 293T cells were transfected with expression vectors for either Myc-FOXO4-TM, Myc-FOXO4-TM-3KR, Myc-FOXO4-TM-K237R, Myc-FOXO4-TM-4KR, and HA-p300, as indicated, then subjected to immunoprecipitation with antibody for Myc. The resulting precipitates were subjected to immunoblot analysis with antibodies for Myc and acetyl lysine. (D) COS-7 cells were transfected with the pGL-6xDBE luciferase reporter plasmid, as well as with an expression vector for either myc-tagged FOXO4-TM or FOXO4-TM-4KR in the absence (open bars) or presence (closed bars) of an expression plasmid for HA-p300. The cells were assayed for luciferase activity 24 h after transfection. The expression of p300 proteins is indicated at the top as an insert. Data are mean ± SD of triplicates from an experiment repeated twice with similar results.

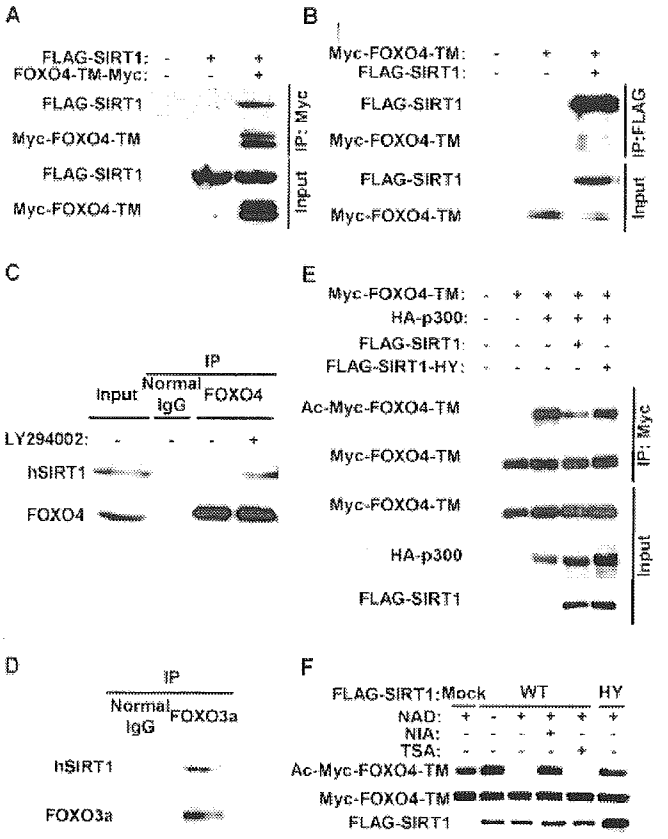

Figure 2. Interaction of mammalian SIRT1 with FOXO4 and SIRT1-mediated FOXO4 deacetylation. (A and B) The 293T cells were transfected with expression vectors for FLAG-SIRT1 and Myc-FOXO4-TM, as indicated. Immunoprecipitates, prepared from transfected cells with antibodies for Myc (A) or FLAG (B), were subjected to immunoblot analysis with antibodies for FLAG (FLAG-SIRT1) or Myc (Myc-FOXO4-TM). Cell lysates (input) were also subjected directly to immunoblot analysis with the same antibodies. (C) Jurkat cells treated (or not) with 20 μM LY294002 for 1 h were lysed and subjected to immunoprecipitation with antibodies for FOXO4 or control IgG, and the resulting precipitates were subjected to immunoblot analysis with antibodies for SIRT1 or FOXO4. (D) Confluent HeLa cells were lysed and subjected to immunoprecipitation with antibodies for FOXO3a or control IgG, and the resulting precipitates were subjected to immunoblot analysis with antibodies for SIRT1 or FOXO3a. (E) The 293T cells were transfected with expression vectors for the indicated proteins and subjected to immunoprecipitation with antibodies for Myc. The resulting precipitates and original cell lysates were subjected to immunoblot analysis with antibodies for acetyl lysine, Myc, FLAG, and α-tubulin. (F) Acetylated Myc-FOXO4-TM from transfected 293T cells coexpressing HA-p300 was incubated in the absence or presence of NAD, nicotinamide (NIA), or trichostatin A (TSA) with FLAG-SIRT1 or FLAG-SIRT1-HY, which had also been immunoprecipitated from transfected 293T cells. The reaction mixtures were immunoprecipitated with antibody for Myc, then subjected to immunoblot analysis with antibodies for acetyl lysine or Myc (upper two panels). The lower panel shows immunoblot analysis with antibodies for FLAG, immunoprecipitated from cells transfected with the SIRT1 expression vectors.

p300-mediated acetylation of FOXO4 negatively regulates its transactivation activity, although p300 is involved in FOXO-mediated transactivation by recruiting the basal transcriptional complex.

SIRT1 interacts and deacetylates FOXO4. Given that SIRT1 functions as an NAD-dependent deacetylase, SIRT1 would counteract p300-mediated inhibition of FOXO4 transactivation activity. To examine this possibility, we first subjected 293T cells to transient transfection with expression vectors for FLAG-tagged wild-type SIRT1 and Myc-FOXO4-TM. Immunoprecipitation and immunoblot analysis of the transfected cells revealed that SIRT1 coprecipitated with FOXO4-TM and vice versa (Fig. 2A and B). To confirm the physiological interaction between endogenous human FOXO4, FOXO3a and SIRT1 proteins, whole cell extracts from Jurkat cells treated with PI-3K inhibitor, LY294002, which induces nuclear accumulation of FOXO4 (6), and from confluent HeLa cells in which FOXO3a accumulated within the nucleus (9), were subjected to immunoprecipitation. Co-immunoprecipitations of FOXO4 and SIRT1, and FOXO3a and SIRT1, were evident in LY294002-treated Jurkat and confluent HeLa cells, respectively (Fig. 2C and D). These results indicate that FOXO4 and FOXO3a proteins form a complex with SIRT1 within the nuclei of mammalian cells.

We next investigated whether SIRT1 catalyzes the deacetylation of FOXO4 *in vivo*. We transfected 293T cells with various combinations of expression vectors for Myc-FOXO4-TM, HA-p300, and FLAG- SIRT1 or SIRT1-HY, a catalytically inactive mutant (14). The acetylation of FOXO4-TM, apparent in cells overexpressing p300, was reduced by coexpression of SIRT1, but not by that of SIRT1-HY (Fig. 2E). The acetylation of FOXO3a-TM, induced by coexpression of

p300, was also reduced by coexpression of SIRT1, but not by that of SIRT1-HY (data not shown). We then examined whether SIRT1 directly deacetylates FOXO4 *in vitro*. Acetylated Myc-FOXO4-TM from transfected 293T cells coexpressing HA-p300 was incubated with FLAG-SIRT1 or FLAG- SIRT1-HY immunoprecipitated from transfected 293T cells. Whereas the immunoprecipitated SIRT1 deacetylated FOXO4-TM in an NAD-dependent manner, SIRT1-HY did not (Fig. 2F). The deacetylation of FOXO4-TM by SIRT1 *in vitro* was prevented by nicotinamide, a specific inhibitor of SIRT1 activity (13), but not affected by trichostatin A, an inhibitor of classical histone deacetylases (HDACs).

SIRT1 enhances FOXO transcriptional activity by NAD-dependent deacetylation. We examined whether the deacetylation of FOXO4 by SIRT1 counteracts the negative regulation of FOXO4 activity by p300-mediated acetylation. We subjected HCT116 cells to transient transfection, both with the pGL-6xDBE reporter plasmid and an expression vector for either FOXO4-TM, then incubated the cells in the absence or presence of various concentrations of resveratrol, a plant polyphenol that increases the NAD-dependent deacetylase activity of SIRT1 (22). The transactivation activities of FOXO4-TM were increased by resveratrol in a dose-dependent manner (Fig. 3A). Conversely, treatment of the cells with nicotinamide resulted in the inhibition of the transactivation activities of FOXO4-TM (Fig. 3B). The transactivation activities of FOXO4 and FOXO4-TM were also increased in a dose-dependent manner by coexpression of SIRT1, but not affected by coexpression of either SIRT1-HY or SIRT3, a mitochondrial member of the Sir2 family (Fig. 3C and D). Moreover, overexpression of SIRT1 increased the transactivation activity of FOXO4-TM, as measured with a luciferase reporter plasmid controlled by the native promoter of human GADD45 (Fig. 3E). Furthermore, the introduction of FOXO4-TM by retroviral gene transfer resulted in the accumulation of p27 as reported (23). The co-introduction of FOXO4-TM with SIRT1, but not SIRT1-HY, led to increased accumulation of p27 (Fig. 3F). These results indicate that SIRT1 increases the transactivation activity of FOXO proteins as a result of its NAD-dependent deacetylation activity.

SIRT1 is essential for FOXO-mediated GADD45 induction in response to oxidative stress. We and others have previously shown that members of FOXO activate the *GADD45* promoter in response to oxidative stress and UV radiation (7,8). FOXO usually localizes in the cytoplasm by PKB phosphorylation leading to 14-3-3 and CRM1-mediated nuclear exclusion in serum containing medium. Therefore, FOXO should be accumulated within the nucleus to activate gene expression as a transcription factor. As reported, the treatment of NIH-FOXO4 cells, in which mouse FOXO4 has been introduced by retroviral-mediated gene transfer, with LY294002 resulted in the accumulation of FOXO4 within the nucleus. In response to oxidative stress, FOXO4 also rapidly accumulated within the nucleus (Fig. 4A). We next examined whether the accumulated FOXO4, in response to oxidative stress, interacts with SIRT1. Whole cell lysates from the NIH-FOXO4 cells, with or without H_2O_2 treatment, were immunoprecipitated with antibody for FOXO4. Co-immunoprecipitations of FOXO4

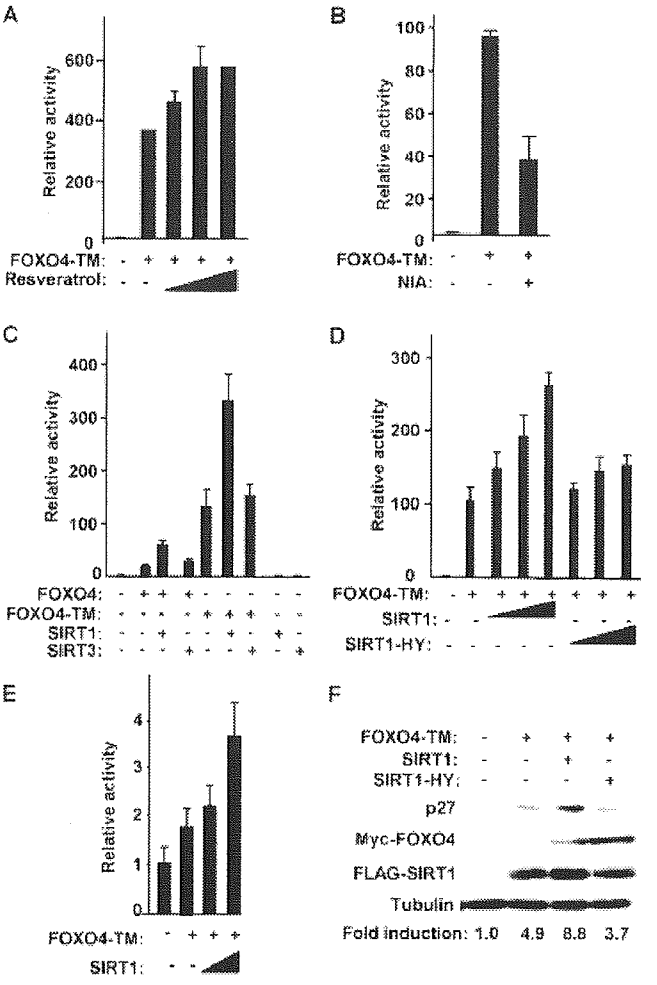

Figure 3. Enhancement of FOXO4 transactivation activity by SIRT1-mediated deacetylation. (A) HCT116 cells were cotransfected with the pGL-6xDBE luciferase reporter plasmid and an expression vector for FOXO4-TM. The transfected cells were incubated for 24 h in the absence or presence (0.5, 1.0, or 2.0 μM) of resveratrol, then assayed for luciferase activity. (B) COS-7 cells were transfected as in (A), incubated for 12 h in the absence or presence of 5 mM nicotinamide, then assayed for luciferase activity. (C and D) COS-7 cells were cotransfected with pGL-6xDBE and expression vectors for FOXO4, FOXO4-TM, SIRT1, SIRT3, and SIRT1-HY, as indicated; the amounts of SIRT1 or SIRT1-HY plasmids were 5, 15, and 30 ng in (D). The cells were assayed for luciferase activity 24 h after transfection. (E) COS-7 cells were cotransfected with pG45-817 (a luciferase reporter plasmid controlled by the *GADD45* promoter) and expression plasmids for FOXO4-TM or SIRT1 (10 or 40 ng), as indicated. Luciferase activity was assayed 24 h after transfection. (A-E) Data are means ± SD of triplicates from experiments repeated at least twice with similar results. (F) Mouse embryonic fibroblast cells were infected with the retrovirus-expressing FOXO4-TM, with or without SIRT1 or SIRT1-HY, cells were lysed and then subjected to immunoblot analysis with antibodies for p27, FLAG (FLAG-SIRT1), Myc (Myc-FOXO4) and α-tubulin. The expression level of p27 was quantified using NIH image analysis software, normalized to α-tubulin, and then indicated as fold induction to the control infectant. Representive data are shown from four independent experiments with similar results.

and SIRT1 were evident in cells treated with H_2O_2 (Fig. 4B). Inhibition by nicotinamide of endogenous SIRT1 activity in NIH-FOXO4 cells treated with LY294002 or H_2O_2 resulted in a small increase in the amount of acetylated FOXO4 (Fig. 4C). Trichostatin A also slightly increased the level of FOXO4 acetylation, whereas treating cells with both nicotinamide and trichostatin A resulted in an additive increase

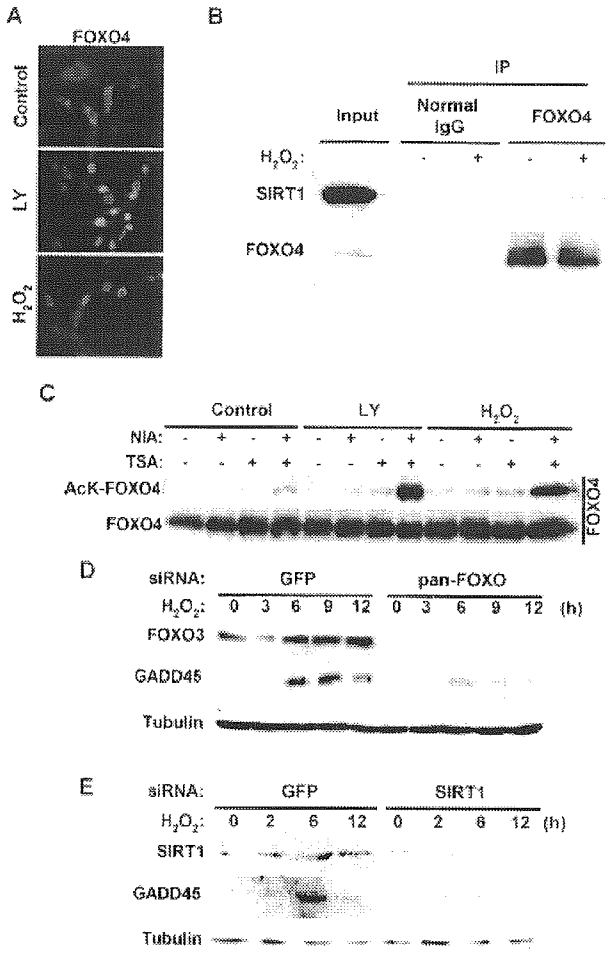

Figure 4. SIRT1 is required for FOXO-mediated GADD45 expression in response to oxidative stress. (A) NIH-FOXO4 cells were treated with 20 μM LY294002 or 1 mM H_2O_2 for 30 min, then fixed with 3% paraformaldehyde in PBS for 15 min, and immunostained with antibody for FOXO4 followed by donkey Cy3-labeled anti-goat IgG antibody, and visualized by fluorescence microscopy. (B) NIH-FOXO4 cells were treated with 1 mM H_2O_2 for 30 min, and subjected to immunoprecipitation with antibodies for FOXO4 or control IgG, and the resulting precipitates were subjected to immunoblot analysis with antibodies for SIRT1 or FOXO4. (C) NIH-FOXO4 cells were incubated for 3 h with 50 μM LY294002 or 1 h with 1 mM H_2O_2 in the absence or presence of nicotinamide (5 mM) or trichostatin A (0.5 μM) as indicated, then subjected to immunoprecipitation with antibodies for FOXO4. The resulting precipitates were subjected to immunoblot analysis with antibodies for acetyl lysine or FOXO4. (D and E) Saos2 cells were transfected with siRNAs specific for GFP (control), pan-FOXO or SIRT1. After 72 h, the cells were treated with 1 mM H_2O_2 for 1 h. Cells were lysed at the indicated times after treatment and subjected to immunoblot analysis with antibodies for FOXO3, SIRT1, GADD45 or α-tubulin.

in the amount of acetylated FOXO4. These observations thus indicated that acetylation and deacetylation of FOXO4 occur physiologically, both the SIRT family and HDACs contribute to FOXO4 deacetylation, and the induction of nuclear accumulation by both LY294002 and H_2O_2 markedly induced the acetylation of FOXO4, although the acetylation was reversed by trichostatin A- and nicotinamide-sensitive deacetylases. To address the contribution of FOXO on the induction of GADD45 in response to oxidative stress, we transfected Saos2 cells with an siRNA for pan-FOXO mRNA (24), then treated them with H_2O_2. Although FOXO3 was highly expressed among the FOXO family, the expression of FOXO4 was not detected by immunoblot analysis in Saos2 cells. FOXO3 expression was suppressed in cells transfected with a pan-FOXO siRNA compared with those in cells transfected with a GFP siRNA as a control. Although GADD45 protein was induced in response to H_2O_2 treatment in control cells, the induction of GADD45 was markedly impaired in cell-depleted FOXO, indicating that FOXO is responsible for GADD45 induction in Saos2 cells in response to oxidative stress (Fig. 4D). To clarify the role of endogenous SIRT1 on FOXO-mediated GADD45 induction in response to oxidative stress, cells depleted of SIRT1 and control cells were treated with 1 mM H_2O_2, then GADD45 induction was monitored by immunoblot analysis. The induction of GADD45 in response to oxidative stress was inhibited in cells depleted of endogenous SIRT1, compared with that in control cells (Fig. 4E). These results demonstrated that SIRT1 is essential for FOXO-mediated GADD45 induction in response to oxidative stress.

Discussion

We have shown that mammalian SIRT1 interacts physically, functionally, and physiologically with FOXO. Furthermore, SIRT1 regulates the transactivation activity of FOXO by catalyzing its deacetylation in an NAD-dependent manner in response to oxidative stress. Similar results have been reported by several groups (25-28). The present study extended these findings, and showed that mammalian FOXO also accumulated within the nucleus in response to oxidative stress, thereby triggering the activation of stress-inducible genes, such as GADD45. While Motta *et al* reported that SIRT1 function represses FOXO activity (25), Brunet *et al* proposed that the effects of deacetylation are target gene-specific, such that the expression of proapoptotic genes is inhibited, while genes that regulate cell cycle arrest and resistance to oxidative stress are increased (26). The present study favors the second hypothesis, i.e. deacetylation of FOXOs results in an increase in transcription of stress-resistant genes such as GADD45. Histone deacetylase has been traditionally associated with the repression of gene expression by deacetylating histone or transcription factors. However, it has been reported that yeast histone deacetylase, Rpd3, is required for gene expression in response to stress by, at least, deacetylating histones and also unidentified molecules (29). Our results indicate that the acetylation of FOXO4 suppresses its transactivation activity, and deacetylation of FOXO4 by SIRT1 counteracts its acetylation-mediated suppression. As depletion of endogenous SIRT1 by siRNA results in impaired FOXO-mediated GADD45 expression in response to oxidative stress, our results suggest that oxidative stress triggers nuclear localization of FOXO family members and induces interaction of FOXO and SIRT1 specifically, thereby leading to the activation of GADD45 expression by deacetylating FOXO and possibly histones, such as yeast Rpd3 does.

Restriction of caloric intake extends life span in a wide variety of organisms, including mammals (30). In yeast, the NAD-dependent activity of SIR2 is essential for this effect, suggesting that caloric restriction regulates SIR2 activity by altering the cellular concentration of NAD or nicotinamide (31). Indeed, an increase in the expression of pyrazinamidase/

nicotinamidase 1 (PNC1), which deaminates nicotinamide and thereby reduces its concentration and activates SIR2, is both necessary and sufficient for life span extension of yeast in response to caloric restriction (32). Furthermore, caloric restriction or mutation of *Rpd3*, both of which extend life span in *Drosophila*, results in a two-fold increase in Sir2 expression (33). It has been reported that caloric restriction in mice also increases SIRT1 expression (34). As calorie-restricted animals routinely have lower levels of insulin and IGF-1 (35), the activity of FOXO family proteins would be increased by prolonged nuclear retention. Together with our present findings, these various observations suggest that FOXO family proteins and SIRT1 may cooperate to extend life span in response to the restriction of caloric intake in mammals.

Acknowledgements

We thank T. Furuyama, T. Sakai, T. Kitamura, R. Eckner, M. Ikeda and A. Fukamizu for the reagents, as well as K. Watanabe for helpful discussion and comments. This work was supported by a Grant-in-Aid for Scientific Research from the Ministry of Education, Culture, Sports, Science, and Technology of Japan, and in part by health science research grants for comprehensive research on aging and health from the Ministry of Health, Labor, and Welfare of Japan and Takeda Science Fundation. Y.F.-H. is a research fellow of the Japan Society for the Promotion of Science.

References

1. Kenyon C, Chang J, Gensch E, Rudner A and Tabtiang R: A *C. elegans* mutant that lives twice as long as wild-type. Nature 366: 461-464, 1993.
2. Friedman DB and Johnson TE: A mutation in the age-1 gene in *Caenorhabditis elegans* lengthens life and reduces hermaphrodite fertility. Genetics 118: 75-86, 1988.
3. Lin K, Dorman JB, Rodan A and Kenyon C: *daf-16*: An HNF-3/forkhead family member that can function to double the life-span of *Caenorhabditis elegans*. Science 278: 1319-1322, 1997.
4. Ogg S, Paradis S, Gottlieb S, Patterson GI, Lee L, Tissenbaum HA and Ruvkun G: The Fork head transcription factor DAF-16 transduces insulin-like metabolic and longevity signals in *C. elegans*. Nature 389: 994-999, 1997.
5. Brunet A, Bonni A, Zigmond MJ, Lin MZ, Juo P, Hu LS, Anderson MJ, Arden KC, Blenis J and Greenberg ME: Akt promotes cell survival by phosphorylating and inhibiting a Forkhead transcription factor. Cell 96: 857-868, 1999.
6. Kops GJ, de Ruiter ND, De Vries-Smits AM, Powell DR, Bos JL and Burgering BM: Direct control of the Forkhead transcription factor AFX by protein kinase B. Nature 398: 630-634, 1999.
7. Tran H, Brunet A, Grenier JM, Datta SR, Fornace AJ Jr, DiStefano PS, Chiang LW and Greenberg ME: DNA repair pathway stimulated by the forkhead transcription factor FOXO3a through the Gadd45 protein. Science 296: 530-534, 2002.
8. Furukawa-Hibi Y, Yoshida-Araki K, Ohta T, Ikeda K and Motoyama N: FOXO forkhead transcription factors induce G2-M checkpoint in response to oxidative stress. J Biol Chem 277: 26729-26732, 2002.
9. Kops GJ, Dansen TB, Polderman PE, Saarloos I, Wirtz KW, Coffer PJ, Huang TT, Bos JL, Medema RH and Burgering BM: Forkhead transcription factor FOXO3a protects quiescent cells from oxidative stress. Nature 419: 316-321, 2002.
10. Imai S, Armstrong CM, Kaeberlein M and Guarente L: Transcriptional silencing and longevity protein Sir2 is an NAD-dependent histone deacetylase. Nature 403: 795-800, 2000.
11. Landry J, Sutton A, Tafrov ST, Heller RC, Stebbins J, Pillus L and Sternglanz R: The silencing protein SIR2 and its homologs are NAD-dependent protein deacetylases. Proc Natl Acad Sci USA 97: 5807-5811, 2000.
12. Smith JS, Brachmann CB, Celic I, Kenna MA, Muhammad S, Starai VJ, Avalos JL, Escalante-Semerena JC, Grubmeyer C, Wolberger C and Boeke JD: A phylogenetically conserved NAD^+-dependent protein deacetylase activity in the Sir2 protein family. Proc Natl Acad Sci USA 97: 6658-6663, 2000.
13. Luo J, Nikolaev A, Imai S, Chen D, Su F, Shiloh A, Guarente L and Gu W: Negative control of p53 by Sir2alpha promotes cell survival under stress. Cell 107: 137-148, 2001.
14. Vaziri H, Dessain SK, Ng Eaton E, Imai SI, Frye RA, Pandita TK, Guarente L and Weinberg RA: hSIR2(SIRT1) functions as an NAD-dependent p53 deacetylase. Cell 107: 149-159, 2001.
15. Langley E, Pearson M, Faretta M, Bauer UM, Frye RA, Minucci S, Pelicci PG and Kouzarides T: Human SIR2 deacetylates p53 and antagonizes PML/p53-induced cellular senescence. EMBO J 21: 2383-2396, 2002.
16. Tissenbaum HA and Guarente L: Increased dosage of a sir-2 gene extends lifespan in *Caenorhabditis elegans*. Nature 410: 227-230, 2001.
17. Sakamoto J, Miura T, Shimamoto K and Horio Y: Predominant expression of Sir2alpha, an NAD-dependent histone deacetylase, in the embryonic mouse heart and brain. FEBS Lett 556: 281-286, 2004.
18. Takai H, Naka K, Okada Y, Watanabe M, Harada N, Saito S, Anderson CW, Appella E, Nakanishi M, Suzuki H, Nagashima K, Sawa H, Ikeda K and Motoyama N: Chk2-deficient mice exhibit radioresistance and defective p53-mediated transcription. EMBO J 21: 5195-5205, 2002.
19. North BJ, Marshall BL, Borra MT, Denu JM and Verdin E: The human Sir2 ortholog, SIRT2, is an NAD^+-dependent tubulin deacetylase. Mol Cell 11: 437-444, 2003.
20. Mahmud DL, G-Amlak M, Deb DK, Platanias LC, Uddin S and Wickrema A: Phosphorylation of forkhead transcription factors by erythropoietin and stem cell factor prevents acetylation and their interaction with coactivator p300 in erythroid progenitor cells. Oncogene 21: 1556-1562, 2002.
21. Fukuoka M, Daitoku H, Hatta M, Matsuzaki H, Umemura S and Fukamizu A: Negative regulation of forkhead transcription factor AFX (Foxo4) by CBP-induced acetylation. Int J Mol Med 12: 503-508, 2003.
22. Howitz KT, Bitterman KJ, Cohen HY, Lamming DW, Lavu S, Wood JG, Zipkin RE, Chung P, Kisielewski A, Zhang LL, Scherer B and Sinclair DA: Small molecule activators of sirtuins extend *Saccharomyces cerevisiae* lifespan. Nature 425: 191-196, 2003.
23. Medema RH, Kops GJ, Bos JL and Burgering BM: AFX-like Forkhead transcription factors mediate cell-cycle regulation by Ras and PKB through p27kip1. Nature 404: 782-787, 2000.
24. Hribal ML, Nakae J, Kitamura T, Shutter JR and Accili D: Regulation of insulin-like growth factor-dependent myoblast differentiation by Foxo forkhead transcription factors. J Cell Biol 162: 535-541, 2003.
25. Motta MC, Divecha N, Lemieux M, Kamel C, Chen D, Gu W, Bultsma Y, McBurney M and Guarente L: Mammalian SIRT1 represses forkhead transcription factors. Cell 116: 551-563, 2004.
26. Brunet A, Sweeney LB, Sturgill JF, Chua KF, Greer PL, Lin Y, Tran H, Ross SE, Mostoslavsky R, Cohen HY, Hu LS, Cheng HL, Jedrychowski MP, Gygi SP, Sinclair DA, Alt FW and Greenberg ME: Stress-dependent regulation of FOXO transcription factors by the SIRT1 deacetylase. Science 303: 2011-2015, 2004.
27. Daitoku H, Hatta M, Matsuzaki H, Aratani S, Ohshima T, Miyagishi M, Nakajima T and Fukamizu A: Silent information regulator 2 potentiates Foxo1-mediated transcription through its deacetylase activity. Proc Natl Acad Sci USA 101: 10042-10047, 2004.
28. Van der Horst A, Tertoolen LG, de Vries-Smits LM, Frye RA, Medema RH and Burgering BM: FOXO4 is acetylated upon peroxide stress and deacetylated by the longevity protein hSir2(SIRT1). J Biol Chem 279: 28873-28879, 2004.
29. De Nadal E, Zapater M, Alepuz PM, Sumoy L, Mas G and Posas F: The MAPK Hog1 recruits Rpd3 histone deacetylase to activate osmoresponsive genes. Nature 427: 370-374, 2004.

30. Tissenbaum HA and Guarente L: Model organisms as a guide to mammalian aging. Dev Cell 2: 9-19, 2002.
31. Lin SJ, Defossez PA and Guarente L: Requirement of NAD and SIR2 for life-span extension by calorie restriction in *Saccharomyces cerevisiae*. Science 289: 2126-2128, 2000.
32. Anderson RM, Bitterman KJ, Wood JG, Medvedik O and Sinclair DA: Nicotinamide and PNC1 govern lifespan extension by calorie restriction in *Saccharomyces cerevisiae*. Nature 423: 181-185, 2003.
33. Rogina B, Helfand SL and Frankel S: Longevity regulation by *Drosophila* Rpd3 deacetylase and caloric restriction. Science 298: 1745, 2002.
34. Cohen HY, Miller C, Bitterman KJ, Wall NR, Hekking B, Kessler B, Howitz KT, Gorospe M, de Cabo R and Sinclair DA: Calorie restriction promotes mammalian cell survival by inducing the SIRT1 deacetylase. Science 305: 390-392, 2004.
35. Mobbs CV, Bray GA, Atkinson RL, Bartke A, Finch CE, Maratos-Flier E, Crawley JN and Nelson JF: Neuroendocrine and pharmacological manipulations to assess how caloric restriction increases life span. J Gerontol A Biol Sci Med Sci 56: 34-44, 2001.

Available online at www.sciencedirect.com
SCIENCE DIRECT®
ELSEVIER
Biochemical and Biophysical Research Communications 333 (2005) 427–431
BBRC
www.elsevier.com/locate/ybbrc

Chk2 regulates transcription-independent p53-mediated apoptosis in response to DNA damage ☆

Chen Chen [a], Shigeomi Shimizu [b], Yoshihide Tsujimoto [b], Noboru Motoyama [a,*]

[a] *Department of Geriatric Research, National Institute for Longevity Sciences, National Center for Geriatrics and Gerontology, Obu, Aichi 474-8522, Japan*
[b] *Department of Post-Genomics Diseases, Osaka University Medical School, Suita, Osaka 565-0871, Japan*

Received 17 May 2005
Available online 2 June 2005

Abstract

The tumor suppressor protein p53 plays a central role in the induction of apoptosis in response to genotoxic stress. The protein kinase Chk2 is an important regulator of p53 function in mammalian cells exposed to ionizing radiation (IR). Cells derived from *Chk2*-deficient mice are resistant to the induction of apoptosis by IR, and this resistance has been thought to be a result of the defective transcriptional activation of p53 target genes. It was recently shown, however, that p53 itself and histone H1.2 translocate to mitochondria and thereby induces apoptosis in a transcription-independent manner in response to IR. We have now examined whether Chk2 also regulates the transcription-independent induction of apoptosis by p53 and histone H1.2. The reduced ability of IR to induce p53 stabilization in Chk2-deficient thymocytes was associated with a marked impairment of p53 and histone H1 translocation to mitochondria. These results suggest that Chk2 regulates the transcription-independent mechanism of p53-mediated apoptosis by inducing stabilization of p53 in response to IR.

Keywords: Apoptosis; Chk2; p53; Histone H1; Mitochondria; Thymocytes; Ionizing radiation; Transcription

The genome of cells is continually damaged by environmental insults such as ultraviolet light and ionizing radiation (IR); by oxidative stress, such as that attributable to reactive oxygen species derived from oxidative metabolism; and, in dividing cells, by errors in DNA replication and mitosis. Maintenance of the integrity of genomic DNA relies on the DNA damage checkpoint, which either halts cell cycle progression to allow cells time to repair DNA damage or triggers apoptosis, depending on the extent of DNA damage and on cell type [1–3]. By acting as a central regulator of cell cycle arrest and apoptosis, the tumor suppressor protein p53 protects cells from malignant transformation. This role has earned p53 the designation of "guardian of the genome" or "gatekeeper of the cell" [4,5]. Among the multiple specific functions of p53, the induction of apoptosis is thought to be especially important in preventing tumor progression [6,7].

Regulation of the abundance and transcriptional regulatory activity of p53 is achieved primarily by posttranscriptional modification, including phosphorylation and acetylation [8]. Exposure of cells to IR activates a signaling pathway that includes sensors of DNA damage, signal transducers, and mediators and which results in the stabilization and activation of p53 [1–3]. We and others have previously shown that Chk2 contributes to p53 stabilization in cells exposed to IR and that Chk2 is a critical regulator of p53 function, given that cells derived from Chk2-deficient mice are defective in the transcriptional induction of p53 target genes at the G_1-S checkpoint [9–11]. In addition to the defect in

☆ *Abbreviations:* IR, ionizing radiation; FITC, fluorescein isothiocyanate.

* Corresponding author. Fax: +81 562 46 8437.
E-mail address: motoyama@nils.go.jp (N. Motoyama).

0006-291X/$ - see front matter © 2005 Elsevier Inc. All rights reserved.
doi:10.1016/j.bbrc.2005.05.126

transcriptional activation of proapoptotic genes such as those for Bax and Noxa, various cell types derived from Chk2-deficient mice, including thymocytes, neurons, and adenoviral E1A-transformed mouse embryonic fibroblasts, are resistant to the induction of p53-mediated apoptosis by IR [9–12].

Translocation of p53 to mitochondria and direct induction of apoptosis [13–16] as well as the p53-dependent release of histone H1.2 from the nucleus and consequent induction of apoptosis [17] have been recently described in cells exposed to IR, although the signaling pathway to leading these translocations remain unclear. Chk2 forms a stable complex with p53 in human cells [18] and phosphorylates human p53 at Ser^{20} (Ser^{23} in mouse) and COOH-terminal fragment including Ser^{366}, Ser^{378}, and Thr^{387} of human p53 [10,19–21]. These observations prompted us to examine whether Chk2 regulates the induction of such transcription-independent apoptosis by p53 and histone H1.2. We now show that the translocation of p53 and histone H1 to mitochondria is markedly reduced in Chk2-deficient cells as a result of the defect in p53 stabilization. We therefore conclude that Chk2 regulates both transcription-independent and transcription-dependent mechanisms of p53-mediated apoptosis by stabilizing p53 and by increasing its transcriptional regulatory activity.

Materials and methods

Mice. The generation of Chk2-deficient mice was described previously [9]. The endogenous and disrupted *Chk2* genes were detected by polymerase chain reaction analysis of mouse tail DNA either with 5′-CTCGCTGACCTAGGTAGCAGGACC-3′ and 5′-TGTGCCGG TAGAGGAGCTGG-3′ or with 5′-CTCGCTGACCTAGGTAGCAG GACC-3′ and 5′-GGGTGGGGTGGGATTAGATAAATG-3′ as primers, respectively. The amplification protocol comprised 35 cycles of denaturation for 1 min at 94 °C, annealing for 90 s at 64 °C, and elongation for 90 s at 72 °C. Mice deficient in p53 were obtained from Taconic (Taconic, Germantown, NY).

X-irradiation of cells. Freshly isolated thymocytes from mice of the indicated genotypes were suspended in RPMI 1640 medium supplemented with 10% fetal bovine serum. They were exposed to the indicated dose of X-radiation at a rate of 4.53 Gy/min and then cultured for the indicated times under a humidified atmosphere of 6% CO_2 at 37 °C.

Apoptosis assay. Apoptosis in irradiated thymocytes was assayed with the use of an Annexin V-FITC Apoptosis Detection Kit (Sigma, St. Louis, MO). In brief, harvested cells were washed with ice-cold phosphate-buffered saline, resuspended in 1× binding buffer [10 mM Hepes–NaOH (pH 7.5), 140 mM NaCl, and 2.5 mM $CaCl_2$] at a density of 1.0×10^6 cells/ml, and then incubated for 10 min with fluorescein isothiocyanate (FITC)-conjugated annexin V. The proportion of cells positive for staining by annexin V-FITC was determined immediately thereafter by flow cytometry with a FACScalibur instrument and data analysis with CELL Quest software (BD Pharmingen, San Diego, CA).

Immunoblot analysis. Cells were lysed in a solution containing 50 mM Hepes–NaOH (pH 8.0), 150 mM NaCl, 25 mM EGTA, 1 mM EDTA, 0.1% Tween 20, 10% glycerol, 0.1 M NaF, and a mixture of protease inhibitors (Complete-Mini; Roche, Mannheim, Germany). The protein concentration of the lysates was determined with the BCA protein assay reagent (Pierce, Rockford, IL), after which samples (10 μg of protein) were subjected to SDS–polyacrylamide gel electrophoresis and immunoblot analysis with mouse monoclonal antibodies to mouse p53 (IMX25; Novocastra, Newcastle, UK) or to γ-tubulin (GTU-88, Sigma) or with rabbit polyclonal antibodies to Puma (Pro-Sci, Poway, CA). Immune complexes were detected with horseradish peroxidase-conjugated secondary antibodies and the ECL Plus system (Amersham Bioscience, Piscataway, NJ).

Isolation of mitochondria. Mitochondria were isolated with the use of a Mitochondria/Cytosol Fractionation Kit (BioVision, Mountain View, CA). In brief, thymocytes were washed with ice-cold phosphate-buffered saline, resuspended in 1 ml of 1× cytosol extraction buffer mix containing dithiothreitol and protease inhibitor cocktail, and then incubated for 10 min on ice. The cells were disrupted by 60 strokes of a Dounce homogenizer to yield a crude extract, which was then centrifuged at 700*g* for 10 min at 4 °C. The resulting supernatant was centrifuged at 10,000*g* for 30 min at 4 °C, and the final pellet was washed twice with 1× cytosol extraction buffer mix and saved as the mitochondrial fraction. Protein concentration was determined with a Dc Protein Assay Kit (Bio-Rad, Hercules). The crude extract and mitochondrial fraction were solubilized in SDS sample buffer and then subjected to SDS–polyacrylamide gel electrophoresis and immunoblot analysis with mouse monoclonal antibodies to mouse p53 or to histone H1 (AE-4; Santa Cruz Biotechnology, Santa Cruz, CA). The purity of the mitochondrial fraction was assessed by immunoblot analysis with a mouse monoclonal antibody (20EB; Molecular Probes, Eugene OR) to OxPhos complex IV subunit IV (COX4) and rabbit polyclonal antibodies (FL-261, Santa Cruz Biotechnology) to proliferating cell nuclear antigen (PCNA), as markers for mitochondria and the nucleus, respectively.

Results and discussion

Accumulation of Puma and translocation of both p53 and histone H1 coincide with the initiation of apoptosis

The tumor suppressor p53 induces apoptosis by transcription-dependent and transcription-independent mechanisms in response to exposure of cells to IR. Although the transcriptional activation of p53 target genes for proapoptotic proteins such as Puma is relatively rapid, the accumulation of these proteins to a level sufficient to mediate apoptosis presumably requires additional time. We therefore first examined the kinetics both of the induction of apoptosis and of the expression of Puma in thymocytes exposed to IR. Apoptotic cells were detected 3 h after X-irradiation and their percentage increased thereafter (Fig. 1A). Although p53 was stabilized within 1 h after X-irradiation, Puma accumulation was not apparent until 3 h (Fig. 1B), indicating that the accumulation of Puma is coincident with the initiation of apoptosis. We next examined the kinetics of the translocation of p53 and histone H1 to mitochondria. Translocation of both p53 and histone H1 to mitochondria was detected 3 h after X-irradiation of thymocytes (Fig. 1C). Together, these results thus indicated that both transcription-dependent and transcription-independent pathways contribute to the initiation of p53-mediated apoptosis in thymocytes exposed to IR.

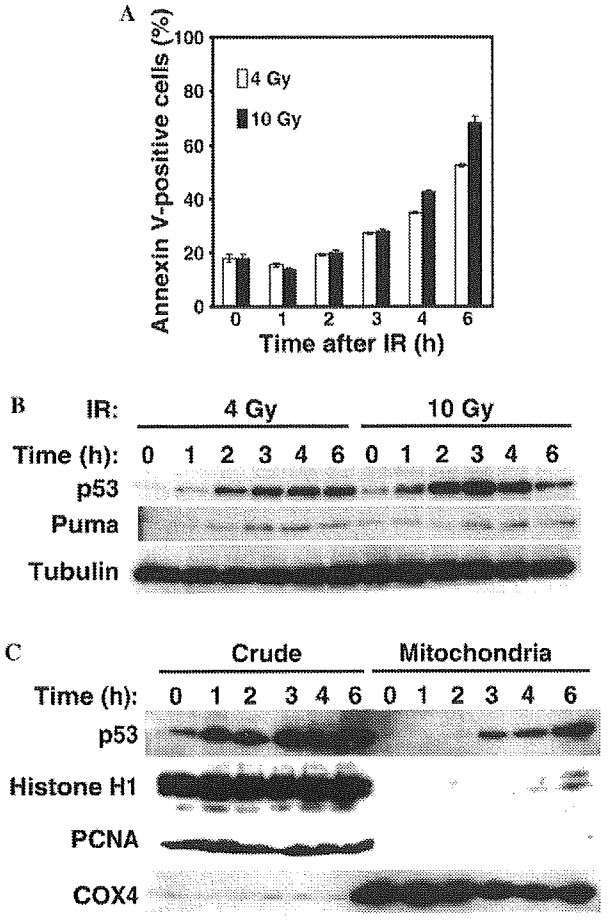

Fig. 1. Kinetics of apoptosis, Puma expression, and translocation of p53 and histone H1 to mitochondria in thymocytes exposed to IR. (A) Thymocytes from wild-type mice were exposed (or not) to 4 or 10 Gy of X-radiation and then cultured for the indicated times before staining with annexin V-FITC and determination of the percentage of annexin V-positive cells by flow cytometry. Data are means ± SD of triplicates from an experiment that was performed a total of two times with similar results. (B) Total cell lysates prepared from thymocytes at the indicated times after exposure to IR (4 or 10 Gy) were subjected to immunoblot analysis with antibodies to mouse p53, to Puma, and to γ-tubulin (loading control). (C) Mitochondrial fractions were purified from thymocytes at the indicated times after exposure to IR (10 Gy). Both total crude extracts (10 μg of protein) and purified mitochondria (10 μg of protein) were subjected to immunoblot analysis with antibodies to mouse p53, to histone H1, to PCNA, and to COX4.

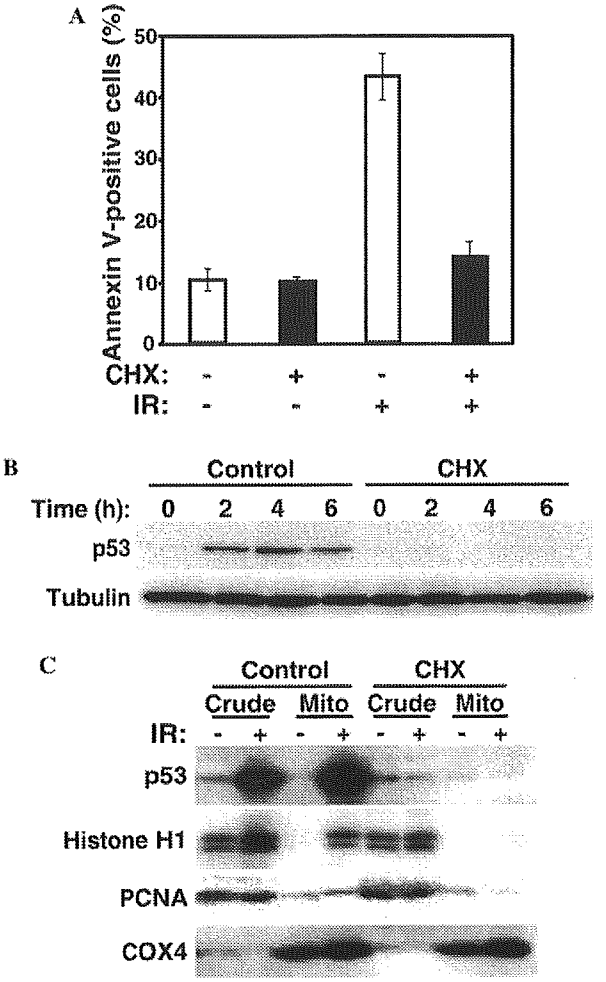

Fig. 2. Inhibitory effects of cycloheximide on p53 stabilization and apoptosis induced by IR. (A) Freshly isolated thymocytes from wild-type mice were incubated with or without cycloheximide (CHX, 10 μg/ml) for 30 min, exposed to 10 Gy of X-radiation, and incubated for an additional 5 h in the continued presence of cycloheximide. The cells were then stained with annexin V-FITC and analyzed by flow cytometry. Data are means ± SD of triplicates from an experiment that was performed a total of two times with similar results. (B) Thymocytes were treated with cycloheximide and irradiated as in (A) and were then lysed at the indicated times after irradiation. Whole cell extracts (10 μg of protein) were subjected to immunoblot analysis with antibodies to the indicated proteins. (C) Thymocytes from wild-type mice were treated with cycloheximide and irradiated as in (A). After incubation of the cells for an additional 4 h, mitochondria (Mito) were isolated and subjected together with total crude extracts (10 μg of protein in each case) to immunoblot analysis with antibodies to the indicated proteins.

Stabilization of p53 is essential for IR-induced histone H1 translocation and apoptosis

The previous observation that IR triggered apoptosis in E1A-transformed mouse embryonic fibroblasts in the presence of the protein synthesis inhibitor cycloheximide indicated that a latent p53 is able to induce apoptosis in a transcription-independent manner [12,22]. We therefore examined whether p53 also induces apoptosis in thymocytes in the presence of cycloheximide. Cycloheximide treatment inhibited the increase in the number of annexin V-positive cells induced by IR (Fig. 2A). The IR-induced accumulation of p53 in thymocytes was also prevented, with the amount of p53 actually decreasing to below the basal level, in cycloheximide-treated thymocytes (Fig. 2B). The amount of p53 protein is still high at basal level in E1A-transformed MEF compared to that of thymocytes in which p53 protein almost is not detectable. These observations indicate that in contrast to E1A-transformed MEFs, stabilization of p53 is essential for IR-induced apoptosis in thymocytes.

We next examined whether cycloheximide also inhibited the translocation of histone H1 to mitochondria in wild-type thymocytes. Isolation of mitochondria at this time revealed that the translocation of neither p53 nor histone H1 to mitochondria was apparent in the cycloheximide-treated cells (Fig. 2C). These data thus indicated that p53 stabilization is essential for the IR-induced translocation of both p53 and histone H1 to mitochondria as well as for IR-induced apoptosis.

Chk2 regulates p53 and histone H1 translocation by stabilizing p53

Thymocytes derived from Chk2-deficient mice were markedly resistant to the induction of apoptosis by IR compared with those from wild-type mice (Fig. 3A). To examine whether Chk2 also regulates the translocation of p53 and histone H1 to mitochondria in response to IR, we exposed thymocytes derived from wild-type or Chk2-deficient mice to X-radiation and isolated the mitochondrial fraction at various times thereafter. Immunoblot analysis revealed that irradiation of wild-type thymocytes increased both the amount of p53 in the crude extract and mitochondrial fraction as well as

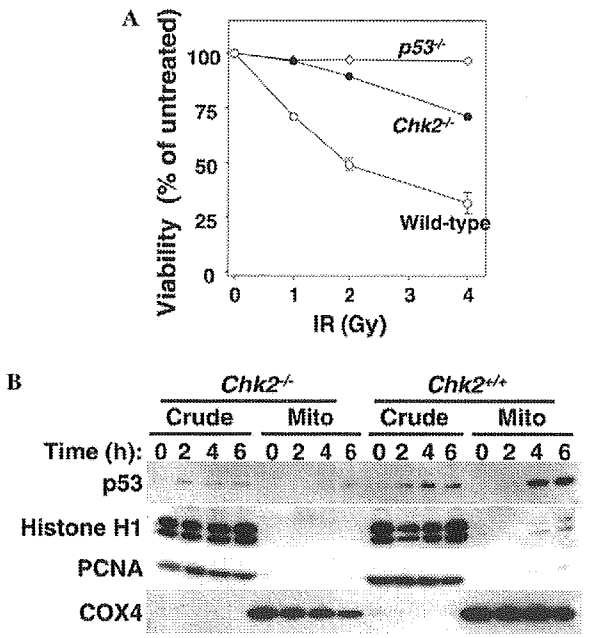

Fig. 3. Resistance to IR-induced apoptosis and impaired translocation of p53 and histone H1 to mitochondria in Chk2-deficient thymocytes. (A) Thymocytes derived from wild-type, Chk2-deficient, or p53-deficient mice were exposed to the indicated doses of X-radiation and incubated for 24 h and analysis by flow cytometry. Data are means ± SD of triplicates from an experiment that was performed a total of two times with similar results. (B) Mitochondrial fractions were isolated from thymocytes of wild-type or Chk2-deficient mice at the indicated times after exposure to IR (10 Gy). Both total crude extracts (10 μg of protein) and mitochondria (10 μg of protein) were subjected to immunoblot analysis with antibodies to the indicated antibodies.

that of histone H1 in the mitochondrial fraction (Fig. 3B). In contrast, the IR-induced stabilization of p53 was impaired in Chk2-deficient thymocytes and the extent of the IR-induced translocation of both p53 and histone H1 to mitochondria was markedly reduced (Fig. 3B). Together, these results indicated that apoptosis mediated by translocation of p53 and histone H1 to mitochondria in response to IR is also impaired in Chk2-deficient thymocytes as a result of the defective stabilization of p53.

The tumor suppressor protein p53 performs multiple functions related to cell cycle checkpoints, apoptosis, and cellular senescence [4,5]. Among these functions, induction of apoptosis has been thought to be the most important for suppression of tumorigenesis [6,7]. The p53 protein induces apoptosis by transcription-dependent and transcription-independent mechanisms [23], the latter being mediated by translocation of p53 and histone H1.2 to mitochondria [13–17]. It remains unknown whether posttranslational modification of p53 is required for its IR-induced mitochondrial translocation, although other functions of p53 are regulated by phosphorylation [8]. We have now shown that Chk2 regulates the transcription-independent mechanism of p53-mediated apoptosis as well as the transcription-dependent mechanism [9–11] in thymocytes exposed to IR. Although the amount of p53 that translocated to mitochondria in response to IR was greatly reduced in Chk2-deficient thymocytes, this effect appeared to be attributable to the lack of p53 stabilization in these cells rather than to a requirement of Chk2 for such translocation per se.

The p53 protein was previously shown to be required for the release of histone H1.2 from the nucleus in response to IR [17]. The IR-induced translocation of histone H1 to mitochondria was also reduced in extent in thymocytes derived from Chk2-deficient mice compared with that in wild-type cells. Furthermore, the amounts of p53 and histone H1 that translocated to mitochondria appeared well correlated with each other, suggesting that the stabilization (and translocation) of p53 determines the efficiency of histone H1 translocation. Together, our observations indicate that, in addition to its regulation of the transcription-dependent mechanism of p53-mediated apoptosis, Chk2 regulates IR-induced apoptosis in thymocytes by increasing the stability of p53, which in turn allows the translocation of accumulated p53 as well as that of histone H1 to mitochondria.

Genetic studies in mice have shown that Chk2 plays an important role in regulation of p53 functions, especially in the induction of apoptosis in response to IR [9–12]. Chk2 was recently shown to collaborate with Brca1 in tumorigenesis [24]. Brca1 has pleiotropic functions, contributing to homologous recombination repair [25], transcription-coupled repair [26], and activation of

the G_2-M cell cycle checkpoint [27,28]. Although the defective differentiation and proliferation of Brca1-deficient thymocytes are rescued by the defect in apoptosis conferred by deficiency of Chk2, the double deficiency leads to the onset of thymic lymphoma in mice [24]. Our present data therefore indicate that Chk2 functions as a tumor suppressor by regulating both transcription-dependent and transcription-independent mechanisms of p53-mediated apoptosis.

Acknowledgments

We thank member of Geriatric Research for discussions. This work was supported by a Grant-in-Aid for Scientific Research on Priority Areas from the Ministry of Education, Culture, Sports, Science, and Technology of Japan, Health Sciences Research Grants for Comprehensive Research on Aging and Health from the Ministry of Health, Labour, and Welfare of Japan and Takeda Science Foundation.

References

[1] B.B. Zhou, S.J. Elledge, The DNA damage response: putting checkpoints in perspective, Nature 408 (2000) 433–439.
[2] Y. Shiloh, ATM and related protein kinases: safeguarding genome integrity, Nat. Rev. Cancer 3 (2003) 155–168.
[3] N. Motoyama, K. Naka, DNA damage tumor suppressor genes and genomic instability, Curr. Opin. Genet. Dev. 14 (2004) 11–16.
[4] D.P. Lane, Cancer. p53, guardian of the genome, Nature 358 (1992) 15–16.
[5] A.J. Levine, p53, the cellular gatekeeper for growth and division, Cell 88 (1997) 323–331.
[6] C.A. Schmitt, J.S. Fridman, M. Yang, E. Baranov, R.M. Hoffman, S.W. Lowe, Dissecting p53 tumor suppressor functions in vivo, Cancer Cell 1 (2002) 289–298.
[7] H. Symonds, L. Krall, L. Remington, M. Saenz-Robles, S. Lowe, T. Jacks, T. Van Dyke, p53-dependent apoptosis suppresses tumor growth and progression in vivo, Cell 78 (1994) 703–711.
[8] E. Appella, C.W. Anderson, Post-translational modifications and activation of p53 by genotoxic stresses, Eur. J. Biochem. 268 (2001) 2764–2772.
[9] H. Takai, K. Naka, Y. Okada, M. Watanabe, N. Harada, S. Saito, C.W. Anderson, E. Appella, M. Nakanishi, H. Suzuki, K. Nagashima, H. Sawa, K. Ikeda, N. Motoyama, Chk2-deficient mice exhibit radioresistance and defective p53-mediated transcription, EMBO J. 21 (2002) 5195–5205.
[10] A. Hirao, Y.Y. Kong, S. Matsuoka, A. Wakeham, J. Ruland, H. Yoshida, D. Liu, S.J. Elledge, T.W. Mak, DNA damage-induced activation of p53 by the checkpoint kinase Chk2, Science 287 (2000) 1824–1827.
[11] A. Hirao, A. Cheung, G. Duncan, P.M. Girard, A.J. Elia, A. Wakeham, H. Okada, T. Sarkissian, J.A. Wong, T. Sakai, E. De Stanchina, R.G. Bristow, T. Suda, S.W. Lowe, P.A. Jeggo, S.J. Elledge, T.W. Mak, Chk2 is a tumor suppressor that regulates apoptosis in both an ataxia telangiectasia mutated (ATM)-dependent and an ATM-independent manner, Mol. Cell. Biol. 22 (2002) 6521–6532.
[12] M.T. Jack, R.A. Woo, A. Hirao, A. Cheung, T.W. Mak, P.W. Lee, Chk2 is dispensable for p53-mediated G1 arrest but is required for a latent p53-mediated apoptotic response, Proc. Natl. Acad. Sci. USA 99 (2002) 9825–9829.
[13] M. Mihara, S. Erster, A. Zaika, O. Petrenko, T. Chittenden, P. Pancoska, U.M. Moll, p53 has a direct apoptogenic role at the mitochondria, Mol. Cell 11 (2003) 577–590.
[14] P. Dumont, J.I. Leu, A.C. Della Pietra 3rd, D.L. George, M. Murphy, The codon 72 polymorphic variants of p53 have markedly different apoptotic potential, Nat. Genet. 33 (2003) 357–365.
[15] J.E. Chipuk, T. Kuwana, L. Bouchier-Hayes, N.M. Droin, D.D. Newmeyer, M. Schuler, D.R. Green, Direct activation of Bax by p53 mediates mitochondrial membrane permeabilization and apoptosis, Science 303 (2004) 1010–1014.
[16] J.I. Leu, P. Dumont, M. Hafey, M.E. Murphy, D.L. George, Mitochondrial p53 activates Bak and causes disruption of a Bak-Mcl1 complex, Nat. Cell Biol. 6 (2004) 443–450.
[17] A. Konishi, S. Shimizu, J. Hirota, T. Takao, Y. Fan, Y. Matsuoka, L. Zhang, Y. Yoneda, Y. Fujii, A.I. Skoultchi, Y. Tsujimoto, Involvement of histone H1.2 in apoptosis induced by DNA double-strand breaks, Cell 114 (2003) 673–688.
[18] J. Falck, C. Lukas, M. Protopopova, J. Lukas, G. Selivanova, J. Bartek, Functional impact of concomitant versus alternative defects in the Chk2-p53 tumour suppressor pathway, Oncogene 20 (2001) 5503–5510.
[19] N.H. Chehab, A. Malikzay, M. Appel, T.D. Halazonetis, Chk2/hCds1 functions as a DNA damage checkpoint in G(1) by stabilizing p53, Genes Dev. 14 (2000) 278–288.
[20] S.Y. Shieh, J. Ahn, K. Tamai, Y. Taya, C. Prives, The human homologs of checkpoint kinases Chk1 and Cds1 (Chk2) phosphorylate p53 at multiple DNA damage-inducible sites, Genes Dev. 14 (2000) 289–300.
[21] Y.H. Ou, P.H. Chung, T.P. Sun, S.Y. Shieh, p53 C-terminal phosphorylation by CHK1 and CHK2 participates in the regulation of DNA-damage-induced C-terminal acetylation, Mol. Biol. Cell (2005).
[22] R.A. Woo, M.T. Jack, Y. Xu, S. Burma, D.J. Chen, P.W. Lee, DNA damage-induced apoptosis requires the DNA-dependent protein kinase, and is mediated by the latent population of p53, EMBO J. 21 (2002) 3000–3008.
[23] J.J. Manfredi, p53 and apoptosis: it's not just in the nucleus anymore, Mol. Cell 11 (2003) 552–554.
[24] J.P. McPherson, B. Lemmers, A. Hirao, A. Hakem, J. Abraham, E. Migon, E. Matysiak-Zablocki, L. Tamblyn, O. Sanchez-Sweatman, R. Khokha, J. Squire, M.P. Hande, T.W. Mak, R. Hakem, Collaboration of Brca1 and Chk2 in tumorigenesis, Genes Dev. 18 (2004) 1144–1153.
[25] M.E. Moynahan, J.W. Chiu, B.H. Koller, M. Jasin, Brca1 controls homology-directed DNA repair, Mol. Cell 4 (1999) 511–518.
[26] L.C. Gowen, A.V. Avrutskaya, A.M. Latour, B.H. Koller, S.A. Leadon, BRCA1 required for transcription-coupled repair of oxidative DNA damage, Science 281 (1998) 1009–1012.
[27] J.S. Larson, J.L. Tonkinson, M.T. Lai, A BRCA1 mutant alters G2-M cell cycle control in human mammary epithelial cells, Cancer Res. 57 (1997) 3351–3355.
[28] X. Xu, Z. Weaver, S.P. Linke, C. Li, J. Gotay, X.W. Wang, C.C. Harris, T. Ried, C.X. Deng, Centrosome amplification and a defective G2-M cell cycle checkpoint induce genetic instability in BRCA1 exon 11 isoform-deficient cells, Mol. Cell 3 (1999) 389–395.

ELSEVIER

Bone 37 (2005) 497 – 503

BONE

www.elsevier.com/locate/bone

Ataxia telangiectasia mutated (*Atm*) knockout mice as a model of osteopenia due to impaired bone formation

Akinori Hishiya[a], Masako Ito[b], Hiroyuki Aburatani[c], Noboru Motoyama[d], Kyoji Ikeda[a], Ken Watanabe[a,*]

[a]*Department of Bone and Joint Disease, National Institute for Longevity Sciences (NILS), National Center for Geriatrics and Gerontology (NCGG), 36-3 Gengo, Morioka-cho, Obu, Aichi 474-8522, Japan*

[b]*Department of Radiology, Nagasaki University Hospital, Nagasaki, Japan*

[c]*Department of Cancer Systems Biology, Research Center for Advanced Science and Technology, The University of Tokyo, Tokyo, Japan*

[d]*Department of Geriatric Medicine, NCGG, Obu, Japan*

Received 19 December 2004; revised 11 April 2005; accepted 20 May 2005
Available online 18 July 2005

Abstract

ATM is a member of the PI-3 kinase protein family, encoded by the gene, *ATM*, responsible for ataxia telangiectasia (AT). AT is recognized as a genomic instability syndrome, sharing accelerated senescence symptoms in human and mouse. Here, we present evidence that the bone phenotype of *Atm* knockout (AtmKO) mice is similar to that observed in disuse and/or aging syndromes. A significant decrease in 3-dimensional bone volume fraction (BV/TV) of the fifth lumbar vertebra was observed in AtmKO mice by μCT, compared with heterozygous control mice at 10 weeks of age. Bone histomorphometry revealed that both BFR/BS and Oc.S/BS were significantly decreased in KO mice. To determine the cellular basis of this bone phenotype, we employed in vitro osteoclastogenesis and colony formation assays using bone marrow cells derived from KO and control mice. There was no difference in osteoclast formation in ex vivo cultures. CFU-F was markedly reduced in AtmKO-derived cultures compared with control mice, whereas differentiation of calvaria-derived osteoblasts did not differ between the genotypes. Furthermore, expression levels of IGF1R were significantly decreased, and p38 was aberrantly phosphorylated in marrow stromal cells from AtmKO mice. These results indicate that the pathogenesis of the osteopenic phenotype in AtmKO mice is similar to that of disuse and/or aging syndromes and is caused, at least in part, by a stem cell defect due to lack of IGF signaling.

Keywords: Premature aging syndrome; Animal models; Mesenchymal stem cells; Knockout

Introduction

Much progress has been achieved in our understanding of the pathogenesis of postmenopausal osteoporosis, characterized by accelerated bone resorption [1,2]. On the other hand, the pathophysiology of senile osteoporosis, caused mainly by declining bone-forming capacity, remains an enigma due to the lack of suitable animal models. Although aged (2 to 3 years old) animals are good candidates, natural aging is a complex phenomenon involving a plethora of factors and is difficult to dissect at the molecular level. Recently, genetically engineered mouse models for studying aging and age-related disorders have been developed [3]. Since they are caused by single gene mutations, they provide valuable tools for studying the pathogenesis of senile osteoporosis at the molecular level. For example, osteopenia with reduced bone formation and resorption has been reported in *klotho* (*kl/kl*) and mutant p53-expressing mice [4,5].

Ataxia telangiectasia (AT) is a human premature aging syndrome characterized by neurodegeneration, immune defects, tumor formation, hypersensitivity to ionizing radiation, and genomic instability [6]. The responsible gene, *ATM* (for AT mutated), is a large protein kinase that belongs

* Corresponding author. Fax: +81 562 44 6595.
E-mail address: kwatanab@nils.go.jp (K. Watanabe).

8756-3282/$ - see front matter © 2005 Elsevier Inc. All rights reserved.
doi:10.1016/j.bone.2005.05.012

to the PI-3 kinase family [10,11]. ATM functions in DNA damage checkpoint and oxidative stress responses, thereby playing a central role in the maintenance of genome stability. Mouse models for AT have been generated by knockout of the mouse Atm gene [7–9]. AtmKO mice exhibit radiosensitivity, genomic instability, growth retardation, and lymphoma, recapitulating main features of human AT [7–9]. The bone phenotype, however, has not been defined. Interestingly, mice deficient in Abl, a downstream protein kinase effector of ATM, exhibit an osteopenic phenotype with reduced bone formation [27]. We report here that AtmKO mice show osteopenia as early as 10 weeks of age, when growth retardation is not apparent. Histomorphometric and biochemical analyses revealed impaired bone formation, which may be caused by limited proliferative potential of osteogenic progenitors. Thus, AtmKO mice may provide a suitable model for studying senile osteoporosis.

Materials and methods

Mice

AtmKO mice (129/SvEv-*Atm*^{tm1Awb}) were obtained from Jackson Labs (Bar Harbor, Maine, USA). All generations were from matings of heterozygous parents. Genotyping was performed as described [9,12] with the exception of the primers used to detect the wild type allele. The primer sequences used for genotyping were as follows:

oIMR640, 5′-GCTGCCATACTTGATCAATG-3′
oIMR641, 5′-TCCGAATTTGCAGGAGTTG-3′.

The sequences used were recommended by Jackson Labs. All animal experiments were approved in advance by the Ethics Review Committee for Animal Experimentation of the National Institute for Longevity Sciences and the National Center for Geriatrics and Gerontology.

Bone morphological and histomorphometric analyses

Lumbar vertebrae and tibias were obtained from 6-, 10-, and 14-week-old female and male mice and subjected to morphological analyses ($n = 3 \sim 6$). Microcomputed tomography (μCT) and bone histomorphometry of the vertebrae and tibias, respectively, doubly labeled by calcein, were performed as described previously [13].

CFU assay

Colony forming unit (CFU) assays were conducted according to Jilka et al. [14]. Briefly, bone marrow cells were obtained from femurs or tibias and seeded at 1.5×10^6 (for CFU-F/CFU-ALP) or 2.5×10^6 (for CFU-Ob or CFU-Adip) cells/well in a 6-well plate. For CFU-F and CFU-Ob, the marrow cell cultures were maintained in phenol red-free αMEM containing 15% FCS and 1 mM Asc-2-P; one-half of the medium was replaced every 5 days. For CFU-Adip, the cultures were maintained in phenol red-free αMEM (Invitrogen, Carlsbad, California, USA) containing 15% FCS and MDI (0.5 mM methylisobutylxanthine, 1 μM dexamethasone, 1 μg/ml insulin) for 25–28 days. The cells were cultured for 10 days and then stained for ALP and counterstained with hematoxylin. Colonies of cells containing a minimum of 20 cells were designated as CFU-F, and those positive for ALP activity as CFU-ALP. For CFU-Ob, the cells were maintained for 25–28 days, fixed in 50% ethanol and 18% formaldehyde, and then stained using 2% Alizarin Red. The oil drops in the adipocytic cells were stained by Oil Red-O.

Osteoblastic cell cultures

Osteoblastic cells were isolated from calvarias of neonatal (P2–P3) AtmKO or wild-type mice following the protocol described by Jochum et al. [15] with minor modifications. For alkaline phosphatase (ALP) staining, osteoblastic cells were cultured in 24-well tissue culture plates. After reaching confluency, medium was supplemented with 60 μg/ml ascorbic acid and 10 nM dexamethasone and cultured for 7 more days. ALP staining was performed using a leukocyte alkaline phosphatase staining kit (SIGMA Diagnostics, St. Louis, USA). For ALP activity measurement, cells from the same conditions described above were washed with PBS and sonicated in RIPA buffer (50 mM Tris–HCl (pH 7.5) containing 150 mM NaCl, 1% NP-40, 0.5% sodium deoxycholate, and 0.1% sodium dodecyl sulfate). ALP activity in the lysate was measured using an ALP activity measurement kit (Wako Pure Chemical Industries, Osaka, Japan). The protein content was determined using BCA protein assay reagent (Pierce Chemical Co., Rockford, Illinois, USA).

M-CSF-dependent cell proliferation assay

Bone marrow cells were isolated from AtmKO or control mice, and the erythrocytes in the collected cells were depleted by standard ammonium-chloride lysis. To assess M-CSF-dependent proliferative response, cells (3×10^4) were cultured in flat-bottom 96-well plates for 2 days with various amounts of M-CSF (R&D Systems, Minneapolis, USA). Cultures were pulsed for 24 h with 1 μCi/well of [^{3}H]thymidine, harvested on glass-fiber filters, and the incorporated radioactivity was determined using a beta counter.

In vitro osteoclastogenesis assay

Bone marrow cells were isolated from AtmKO or control mice and incubated in tissue culture plates with αMEM containing 10% FCS. After 4 h in culture, nonadherent cells

were collected and counted. 5×10^5 cells were cultured for 3 days in 24-well tissue culture plates with 10 ng/ml M-CSF and for an additional 3 days in the presence of both 10 ng/ml M-CSF and 10 ng/ml RANKL (R&D Systems). Adherent cells were then fixed with an acetone–citrate–formalin solution (65:27:7) and stained for TRAP using a leukocyte acid phosphatase kit (SIGMA Diagnostics). The number of TRAP-positive multinucleated cells containing more than three nuclei was counted as osteoclasts.

Immunoblot analysis

Adherent cells from bone marrow of AtmKO or control mice were lysed in RIPA buffer containing 2 mM phenyl–methyl–sulfonyl fluoride, 10 mM sodium fluoride, 2 mM sodium vanadate, and proteinase inhibitor cocktail (Complete™, Roche Diagnostics, GmbH Mannheim, Germany). The cell lysates (15 μg each of protein) were subjected to SDS-PAGE, transferred, and then detected with antibodies using ECL-Plus (Amersham-Pharmacia). Anti-p38 (sc-535), anti-IGF1R (sc-713), and anti-c-Abl (sc-131) antibodies were purchased from Santa Cruz Biotechnology, California, USA. Anti-phosphorylated p38 (9211) and anti-tubulin (T5168) were obtained from Cell Signaling Technology (Beverly, Massachusetts, USA) and SIGMA, respectively.

IGF-dependent cell proliferation assay

Bone marrow cells were obtained as described above. The adherent cells were harvested and replated at a density of 5×10^4 cells/well in 96-well plates. After 24-h serum deprivation, the cultures were labeled with [^{3}H]thymidine with or without human recombinant IGF-I (10 ng/ml; Invitrogen). The incorporated [^{3}H] was measured as described.

Statistical analysis

Data are presented as mean ± SD. All data were analyzed by Student's *t* test. Statistical significance was considered at $P < 0.05$, unless otherwise indicated.

Results

Osteopenia due to impaired bone formation in AtmKO mice

To characterize the bone phenotype of Atm homozygous knockout mice with heterozygous littermates as controls, μCT scanning technique was employed. We analyzed 6-, 10-, and 14-week-old animals. At 6 weeks of age, there was no significant decrease in bone mass of AtmKO mice (data not shown). Since ovarian defect, which was possible to affect bone metabolism, was observed in female KO mice [7–9], we focused in the structural data from male animals. As shown in Figs. 1A and B, 3-dimensional bone volume (BV/TV) of the lumbar vertebrae was markedly decreased in AtmKO mice at 10 weeks of age. At this age, there is no significant difference in body weight between AtmKO and littermate control mice (24.8 ± 1.6 versus 21.5 ± 2.4 g). The trabecular number (Fig. 1C) and thickness (Fig. 1D) were also reduced in AtmKO mice compared to control. The difference between KO and control mice was more pronounced at age of 14 weeks, when some KO animals became cachexic.

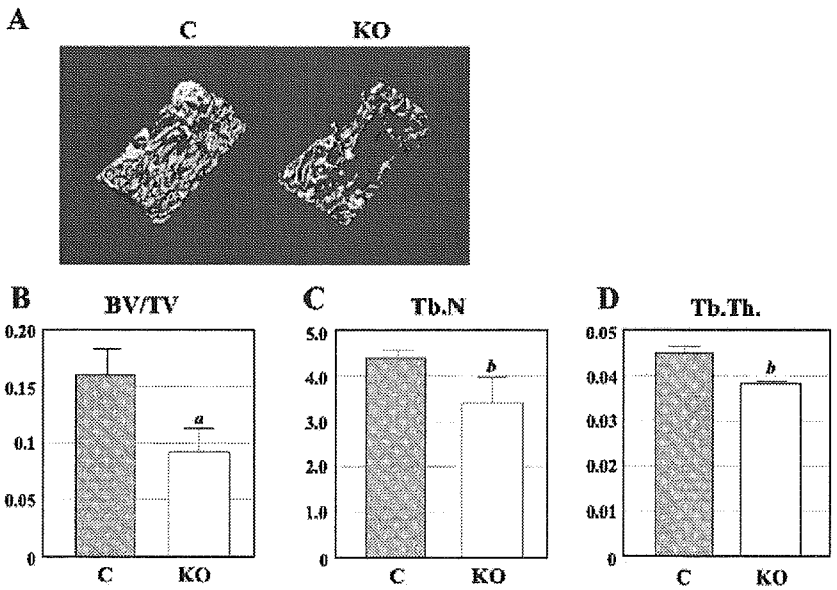

Fig. 1. Micro-CT analysis of lumber vertebrae of AtmKO mice. The fifth lumbar vertebra from heterozygous (C) and knockout (KO) mice were subjected to μCT analysis at 10 weeks of age. (A) Representative 3D images of trabecular architectures are shown. Note that the osteopenic phenotype was observed in knockout mice. (B) Trabecular bone volume fraction (BV/TV); (C) trabecular number (Tb.N); (D) trabecular thickness (Tb.Th.). The data were obtained in male mice. $^aP < 0.005$ and $^bP < 0.05$, significantly different from the respective heterozygous control group.